PERGAMON

Journal of Structural Geology 21 (1999) 1669–1691

JOURNAL OF STRUCTURAL GEOLOGY

www.elsevier.nl/locate/jstrugeo

Compressional- and transpressional-stress pattern for Pliocene and Quaternary brittle deformation in fore arc and intra-arc zones (Andes of Central and Southern Chile)

Alain Lavenu[a, b,*], José Cembrano[b]

[a]*Institut de Recherche pour le Développement (IRD, ex ORSTOM), Casilla 53390, Correo central, Santiago 1, Chile*
[b]*Departamento de Geología, Universidad de Chile, Casilla 13518, Correo 21, Santiago, Chile*

Received 17 August 1998; accepted 7 May 1999

Abstract

Kinematic analysis of fault slip data for stress determination was carried out on Late Miocene to Quaternary rocks from the fore arc and intra-arc regions of the Chilean Andes, between 33° and 46° south latitudes. Studies of Neogene and Quaternary infilling (the Central Depression), as well as plutonic rocks of the North Patagonian Batholith along the Liquiñe–Ofqui Fault Zone, have revealed various compressional and/or transpressional states of stress. In the Pliocene, the maximum compressional stress (σ_1) was generally oriented east–west. During the Quaternary, the deformation was partitioned into two coeval distinctive states of stress. In the fore arc zone, the state of stress was compressional, with σ_1 oriented in a N–S to NNE–SSW direction. In the intra-arc zone the state of stress was transpressional with σ_1 striking NE–SW. Along the coast, in one site (37°30′S) the Quaternary strain deformation is extensional, with an E–W direction, which can be explained by a co-seismic crustal bending readjustment.

1. Introduction

Since the middle Tertiary (25–26 Ma) the central Andes (between 18° and 46°S, a length of 3500 km) has been subjected to convergence of the oceanic Nazca Plate and the continental South American Plate. The subducting Nazca Plate, to the south of Ecuador, is divided into four main segments: two sub-horizontal or flat segments (inclined 5–10°) and two more inclined segments (inclined 30°) (Jordan et al., 1983). The zone under study (Fig. 1) is located above the southernmost segment, with an inclination of 30°. The convergence (42° south latitude–74° east longitude) is of a N 78.8° direction and its average velocity is 7.89 cm/y (DeMets et al., 1994; Tamaki, 1999).

In Chile, from west to east, the Andes present three tectonically distinct parallel domains: (i) a fore arc zone located between the Peru–Chile Trench and the Main Cordillera, in which is found the Coastal Range and longitudinal depressions; (ii) a magmatic arc in the Main Cordillera, which is the active volcanic zone; and (iii) a foreland zone where the most recent deformations are located in Argentina (Costa et al., 1997; Diraison et al., 1998). Several studies (e.g. Barazangi and Isacks, 1976; Bevis and Isacks, 1984; Cahill and Isacks, 1992) have shown that the shape of the oceanic downgoing slab in the region exhibits lateral variations in the dip angle. From north to south the angle of subduction varies and determines different tectonic and volcanic segments. Between 27° and 33°S, the subduction is sub-horizontal and modern volcanism is absent. South of 33°S the angle of subduction increases up to 30° and modern volcanic activity appears as far as 46°30′S (Chilean Ridge Triple Junction) (CTJ). At the 33°S latitude, the main tectonic features of the oceanic plate are the Juan Fernandez Ridge and the aseismic Challenger Fracture Zone. These features delimit plate segments of different ages, the southern one being the

* Corresponding author.
E-mail address: alavenu@dgf.uchile.cl (A. Lavenu)

0191-8141/99/$ - see front matter
PII: S0191-8141(99)00111-X

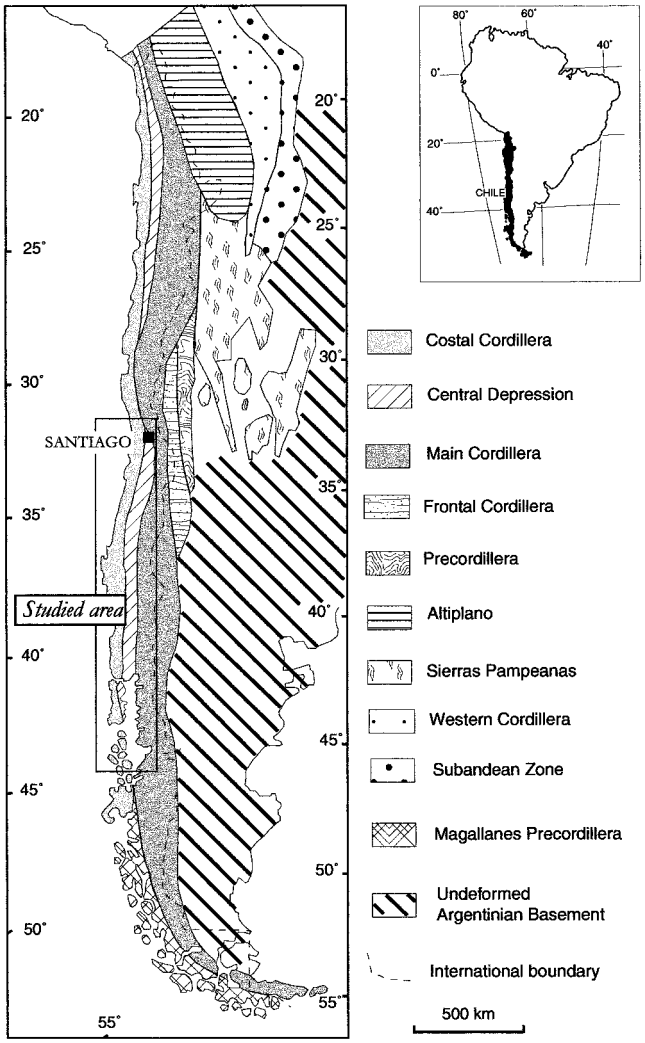

Fig. 1. Morpho-structural units of the Southern Andes. Studied area in the box. Structural provinces of the Southern Andes. This map also shows the limits between the Andean Cordillera and the western edge of the undeformed Argentine basement.

most recent, with a 'normal' 30° dip of the subduction slab, corresponding to the presence of active volcanism (Southern Volcanic Zone of the Andes, SVZA). Current knowledge of the geometry of plate subduction, although partial in the Southern Andes, still allows us to schematically map out a cross-section of the Cordillera at the latitude of 34/36°S (Fig. 2).

The study of geodynamics of the Central and Southern Chilean Andes allows for characterizing the partitioning of the continental deformation of the chain during the oblique convergence of the plates. The objective of this paper is to determine the state of Neogene and Quaternary stress in the Andes of Central Chile. The orientation of stress was established essentially by means of kinematic analysis of faults in the field, as well as through some focal mechanisms of documented earthquakes. Between San Felipe and Aysen 1625 faults at 80 sites were studied. More than 50 independent directions of stress and deformation were obtained. We demonstrate that in the fore arc and intra-arc zones, Pliocene faulting indicates a roughly E–W-trending compression, whereas with respect to the Quaternary, the field data and some focal mechanisms show a stress partitioning with a N–S-trending compression in the fore arc zone and a NE–SW-trending transpression in the intra-arc zone.

2. Geodynamic framework

Between 33° and 46°S the continental fore arc is characterized by the presence of the Coastal Range and a longitudinal valley, the Central Depression, parallel to the Cordillera. This depression starts in the north, in the region of San Felipe (Fig. 3), close to Santiago, and ends to the south of Aysen, in the Ofqui Isthmus, at the latitude of the CTJ. It extends for more than 1000 km, with a width that does not exceed 75 km. Its western limit, with the Coastal Range, is characterized by the presence of eroded fault-line scarps. Its eastern limit, with the Main Cordillera (SVZA) between 33 and 36°S, appears to be marked by the presence of an important eroded fault-line scarp. Between 38° and 46°S, the eastern limit of the Central Depression merges with the volcanic arc along which the Liquiñe–Ofqui Fault Zone (LOFZ) is developed. This fault zone, one of the largest active strike-slip fault zones of modern subduction (e.g. Jarrard, 1986), is characterized by a series of NNE–SSW lineaments, faults and ductile-shear zones along the direction of the Mio-Pliocene and the Recent magmatic arcs. The Liquiñe–Ofqui Fault Zone, a structure extending more than 950 km in length, represents one of the main lineaments of Chile. Its existence was established at the end of the last century (Steffen, 1944 in Hauser, 1991) and little by little understanding of it has evolved (Klohn, 1955, 1960; Moreno and Parada, 1974; Solano, 1978; Hervé et al., 1979). Based on limited field data, this fault was considered dextral (Hervé, 1976, 1977; Hervé and Thiele, 1987). Recently, dextral strike-slip and reverse dip-slip movement on the fault has been clearly established through more detailed studies of ductile shear zones of the Miocene and part of the Pliocene, as well as the brittle dextral strike-slip shear zone from the Pliocene and the Quaternary (Cembrano, 1992; Cembrano and Hervé, 1993; Lavenu and Cembrano, 1994; Cembrano et al., 1996a, b; Lavenu et al., 1997; Cembrano et al., 1997; Cembrano, 1998).

Although the Central Depression and the Main Cordillera are parallel (Fig. 4), the current limit of the Central Depression does not correspond to an active lineament. The northern and southern geographic limits of the Central Depression correspond to the

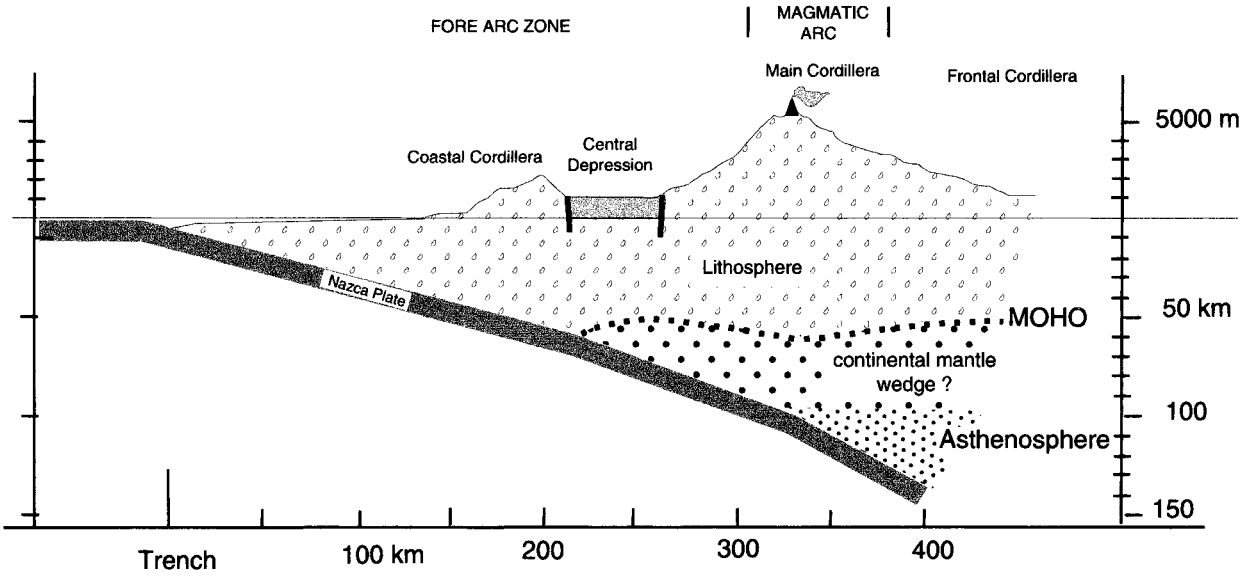

Fig. 2. Cross-sectional sketch across the Nazca–South American plate subduction at 34–36°S.

northermost end of the present SVZA associated with the inclined subducting plate segment. The same applies for the northern Chilean Central Depression between 18 and 27°S. The zone without depression corresponds to the flat slab zone between 27 and 33°S.

The Central Depression was originally described as a graben or half-graben (Aubouin et al., 1973; Laugenie, 1982; Cisternas and Frutos, 1994), nevertheless the present-day geometry and kinematics of its borders do not represent a graben defined by normal faults. The geomorphologic features originated in the Neogene, during which an extensional tectonic event favoured the development of the half-graben. In this case, if there was an active fault between the Central Depression and the Main Cordillera, it would have been before the Quaternary.

The eastern border of the Central Depression is straight, with several indentations. In places, the limit between the Central Depression and the volcanic arc is not exposed, owing to overlying lava flows. Around 36°S, this limit is marked by regional-scale faults of a N 030° direction, in rising steps, caused by the sinking of the Oligo-Miocene volcanic layers, which pass under the filling of the Depression. Measurements of the faults along this scarp in Tertiary rocks show essentially strike-slip movements compatible with E–W and N–S shortening.

The western border of the Central Depression is made up of a system of faults with N–S to N 010° strikes, and oblique faults with N 030° to N 040° strikes. The majority of measured faults along the western border of the Central Depression have strike-slip slickensides (these faults were measured in rocks of various ages, from the Triassic to the Neogene). Some faults show reverse sense of motion (of an indeterminate age). There are also few examples of normal fault striations, which are generally representative of a systematic gravitational collapse directed toward the Central Depression, and have never been interpreted in terms of a well-defined and homogeneous stress field.

Beginning at 35°S and to the east of the Main Cordillera, there is a zone without deformation (or suffering little deformation during the Neogene and Quaternary) which can be defined as part of the 'shield' or Argentine basement (Fig. 1).

Between 39°S and 41°30′S, the part of the Main Cordillera east of the LOFZ appears as an uplifted block. West–east profiles of the Central and Main Cordillera (Fig. 5) at the latitudes of 39°30′S and 41°10′S show, both in terms of landscape and topographical cross-sections, that the Quaternary and/or Plio-Quaternary volcanoes lie over morphological surfaces that are found at different altitudes. To the west of the LOFZ and upon the LOFZ, the main volcanoes, such as Villarrica, El Macho, Quetrupillan (39°30′S) and Osorno (41°10′S) lie on a surface at an average altitude of 1000 m (or less for Mount Osorno). To the east of the LOFZ, where the average surface altitude increases, volcanoes such as Lanín (39°30′S) and Tronador (41°10′S) lie on surfaces with an average altitude of more than 1500 m. Between the two zones there is a difference in altitude of an average of 600–800 m. This difference in altitude can be explained by uplifted blocks of basement of the eastern part of the Main Cordillera ('pop up' as described in Argentina by Diraison et al., 1998).

Between 41°30′S and 46°S, the geological mapping of the Central Depression does not allow one to dis-

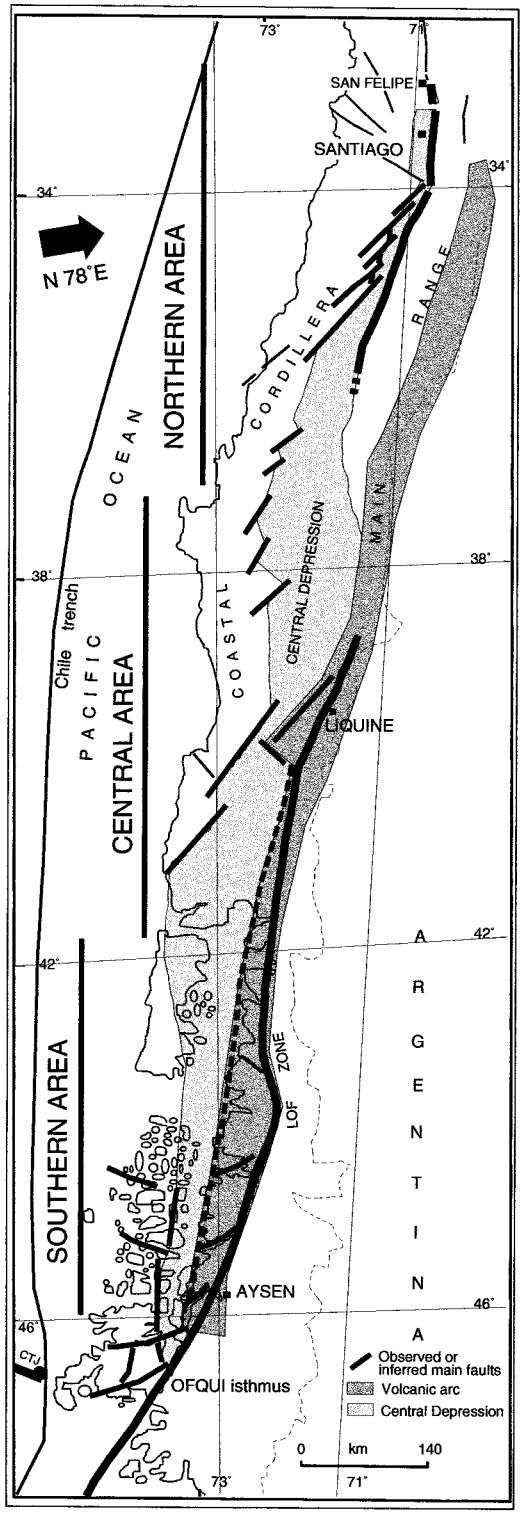

Fig. 3. Simplified structural map of central-southern Chile.

tinguish a well-developed and homogeneous pattern of faults. The Chiloé zone, composed of numerous islands, is not well known geologically. To the east of the Central Depression, the LOFZ forms the western boundary of a very deformed domain with a system of north–south and northeast-trending faults, defining a duplex-like structure (Cembrano et al., 1996a; Cembrano, 1998). South of 46°S, the Central Depression disappears. The LOFZ strikes N 020°, forming the limit between the Coastal Range and the Main Cordillera.

This fore arc zone, and more particularly the Coastal Range, appears to be made up by a number of independent blocks displaced from one another, rather than a coherent coastal sliver (Hervé, 1977; Beck, 1988). The LOFZ constitutes the current rupture zone where dextral displacement of the fore arc and back arc zones occurs (e.g. Nelson et al., 1994). The system of known faults to the west complicates this scheme. The geometry could be interpreted according to the mechanism of small block model proposed by Sylvester (1988) and Nelson and Jones (1987). Although the Cenozoic block rotations have not been studied in enough detail, limited available paleomagnetic data show small counterclockwise rotations west of the LOFZ and small clockwise rotations to the east (e.g. Rojas et al., 1994). It appears that the general disposition of the geometry and geology of this fore arc is better explained with an oblique subduction model (Fitch, 1972; Beck, 1983; Jarrard, 1986; McCaffrey, 1992; Beck et al., 1993) rather than with an indentation model (Forsythe and Nelson, 1985; Nelson et al., 1994). In effect, the latter model does not allow for explaining the deformation along the full length of the LOFZ (Cembrano et al., 1996a, b), although it does explain Pliocene continental deformation close to CTJ (e.g. Cembrano, 1998).

3. Methodology

The region under study, from north of Santiago (32°30′S) to south of Aysen (46°S) was divided into two margin-parallel geological domains: (i) the fore arc domain, including the Coastal Range, the Central Depression and part of the Main Cordillera near Santiago, and (ii) the volcanic arc zone or intra-arc zone.

In the northern area between 32°30′ and 37°S, only the fore arc zone was studied; the intra-arc zone (on the Chilean–Argentinean border) has very limited access and therefore remains without data. Neogene and Quaternary deformations were studied from the Coast to the Main Cordillera. Striated fault planes were measured on rocks of ages varying from the Late Cretaceous/Early Tertiary to the Quaternary.

In the central area between 37° and 42°S, it was possible to study the fore arc and the volcanic arc zones. The analysis was done in the Coast (the Arauco Peninsula and Chiloé Island), in the Central Depression and along the intra-arc LOFZ.

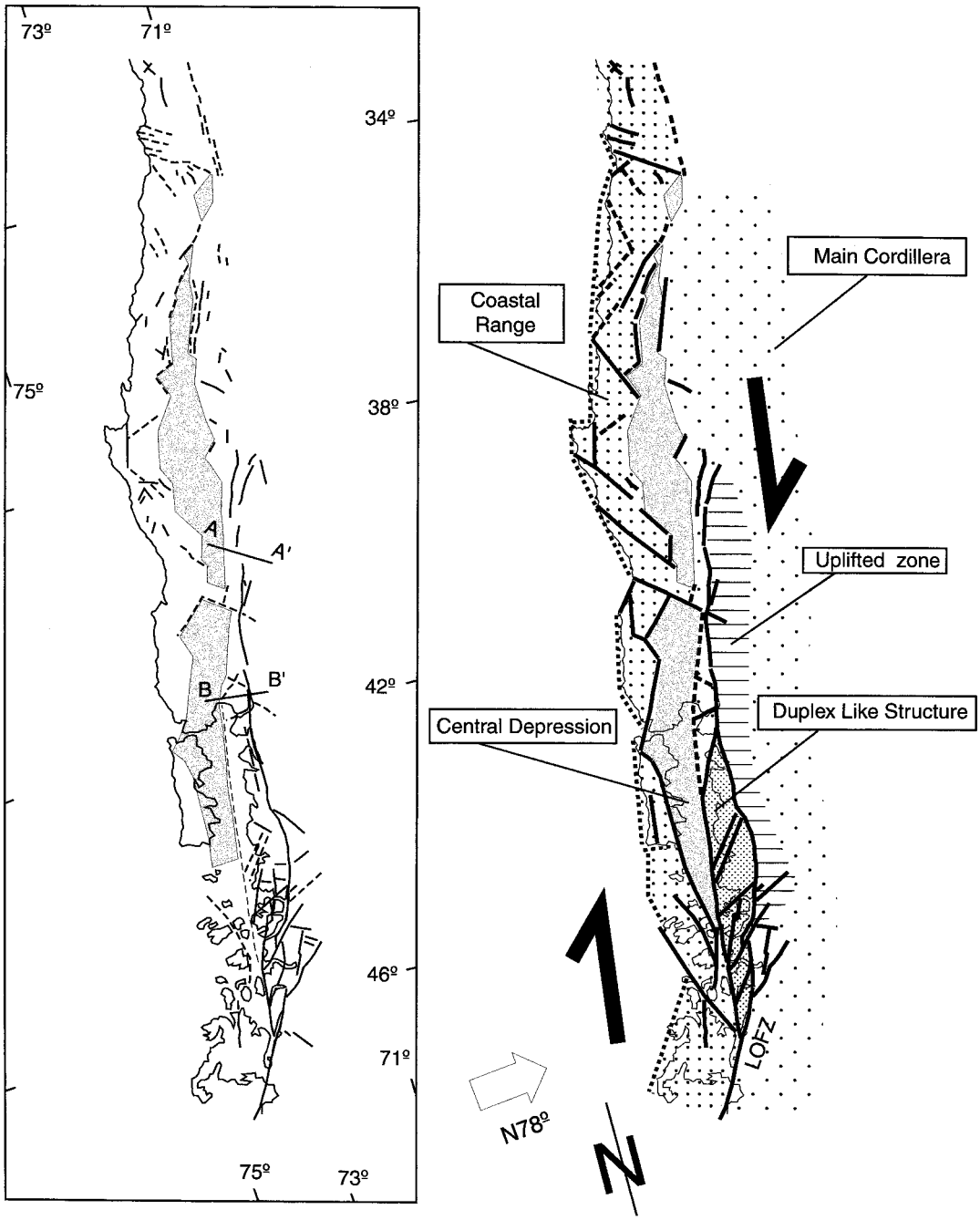

Fig. 4. Strike-slip tectonic zonation in the oblique convergence between the Coast and Main Cordillera. The Coastal Range is fragmented in various blocks. This geometry could be a result of the mechanism of small block model with internal rotation according to Nelson and Jones (1987) and Sylvester (1988). Between 42°S and 47°S, the LOFZ, striking N–S, is characterized by a complex duplex geometry. To the east, uplifted zones take place in the magmatic arc.

Measurements were made in Quaternary sediments (Coastal and Central Depression) and Neogene and Quaternary rocks.

In the southern area between 42° and 46°S, only the volcanic arc zone along the LOFZ was studied. Striated fault planes were measured on Neogene and Quaternary rocks.

In order to determine the state of stress we calculate a stress tensor **T** using an inverse microfault analysis. Since Anderson (1951), Wallace (1951), and Bott (1959), striated slickensides along fault planes are interpreted in term of stresses. The direction of striae is supposed to be collinear to the applied shear stress, depending (i) on the orientation and (ii) on the shape

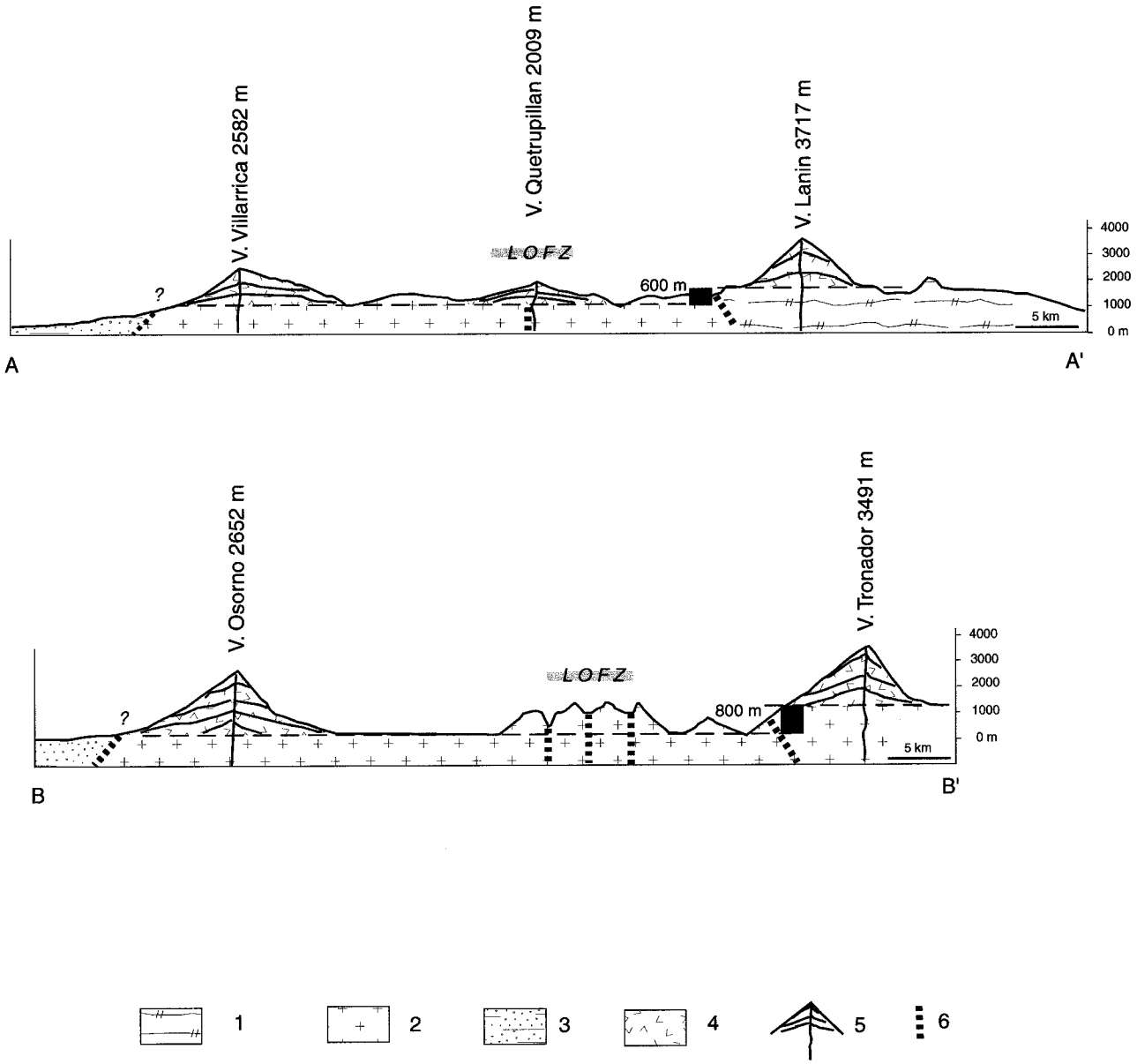

Fig. 5. Morphological profiles across intra arc zone and Liqiñe Ofqui Fault Zone (location in Fig. 4). West of the LOFZ the main volcanoes (Villarrica, Quetrupillan, El Macho, Osorno) lie on a surface at an altitude of 1000 m. East of the LOFZ, the main volcanoes (Lanin, Tronador) lie on an uplifted surface at an altitude of 600–800 m. 1—Middle Mesozoic deposits; 2—Undifferentiated North Patagonian Batholith; 3—Central Depression deposits; 4 and 5—Quaternary volcanoes; 6—Main faults zones.

ratio R of the stress tensor. Carey's inversion algorithm based on least-square techniques (Carey and Brunier, 1974; Carey, 1979) allows for calculating a stress tensor and the three principal components of the stress tensor σ_1, σ_2, σ_3. The different stress regimes (compressional, strike-slip and extensional) are limited by four revolution stress tensors (e.g. Ritz and Taboada, 1993) (Fig. 6) and the stress ellipsoid shape ratio R $[(\sigma_2-\sigma_1)/(\sigma_3-\sigma_1)]$ allows determination of the different types of tensors. For the general microtectonic method, see Carey and Brunier (1974), Sébrier et al. (1985) and Lavenu et al. (1995).

4. Results of the inversion

Based on the analysis of the tensors obtained, it was possible to determine two tectonic events within the three zones:

- a Pliocene event, approximately constrained in time between 4.5 and 1.6 Ma, in every case found to be prior to the Quaternary. This event occurred between 4.5/4.7 Ma and 2.8/3.9 Ma in the northern area, between 8.4 Ma and 3.6 Ma in the central area, and between 5.4 Ma and 1.6 Ma in the southern area;

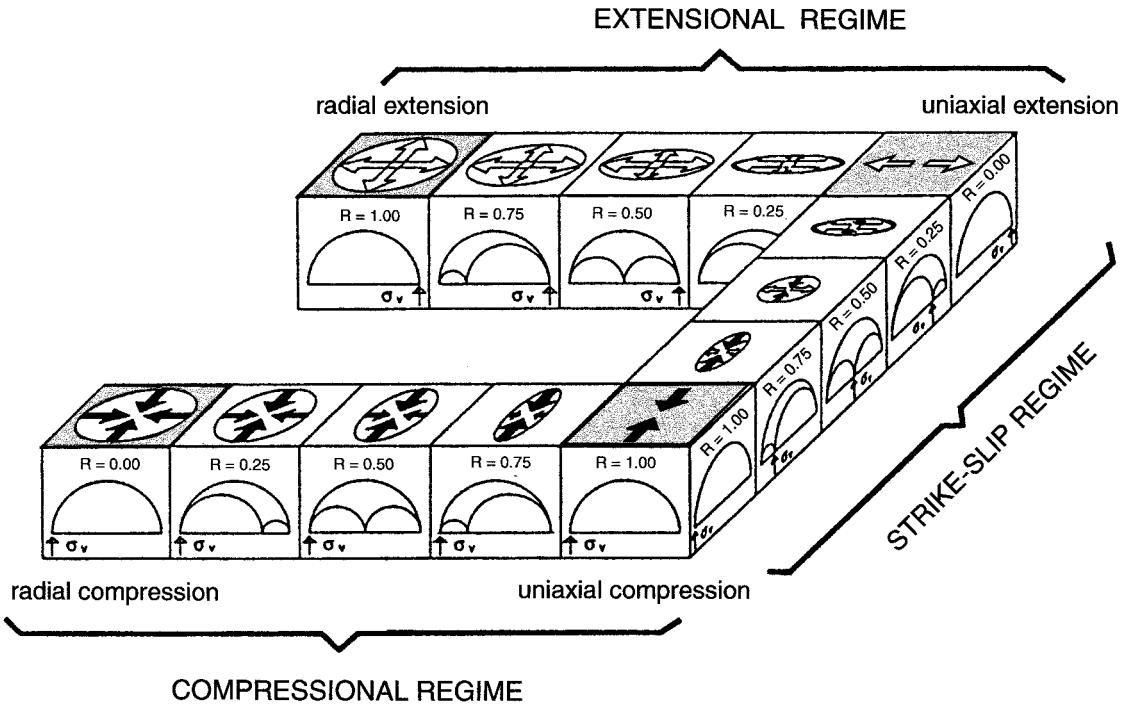

Fig. 6. Classification of different types of stress tensors. The four revolution stress tensors are indicated by shaded squares (modified from Ritz and Taboada, 1993).

- a Quaternary event, later than 2.8 Ma in the northern area, later than 3.6 Ma in the central area, and later than 1.6 Ma in the southern area (Fig. 7).

The sites were analyzed from north to south. The general results are summarized in Tables 1–9 and some sites will be described in detail, four concerning the Pliocene tectonic event (Fig. 8) and five concerning the Quaternary tectonic event (Fig. 9). The ages of the events will be discussed for each zone.

4.1. The Pliocene event

The principal results are presented in Tables 1–4 and Fig. 8. Measurements of striated fault planes in the northern and central areas were taken from the

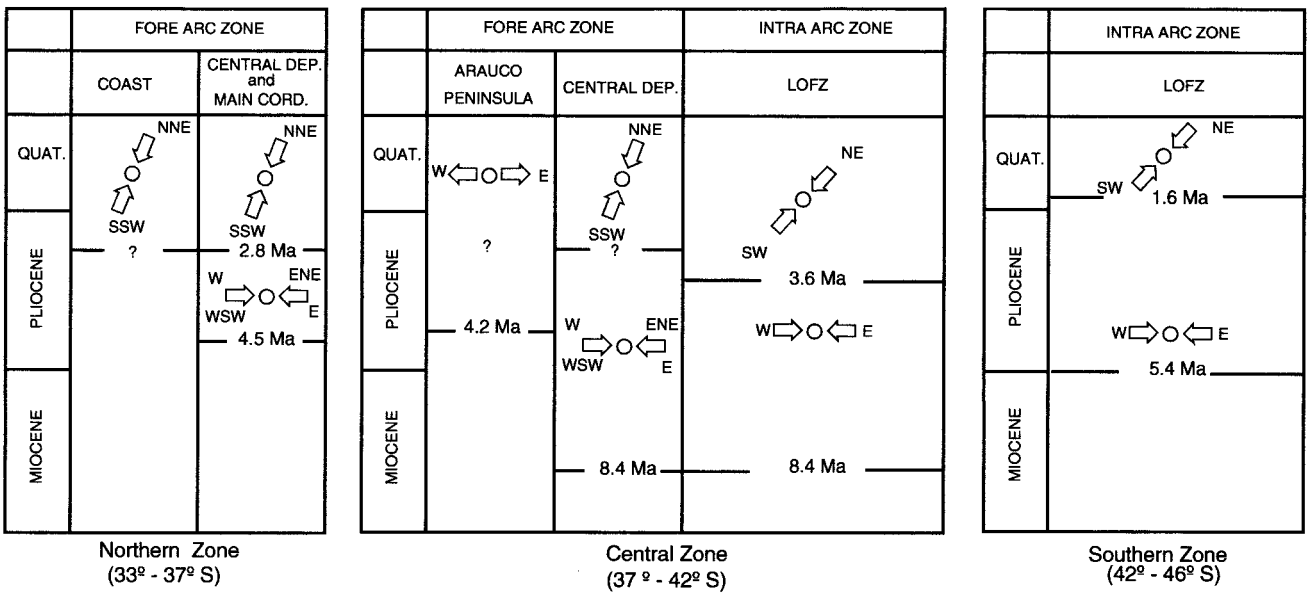

Fig. 7. Chronology and strike of the different tectonic regimes.

Table 1
Parameters of the deviatoric stress tensors computed from the Pliocene faults of the Central Depression and Main Cordillera. Present fore arc zone, northern area

Site	Age of unit	ND	Latitude S	Longitude W	Principal stress directions						R
					σ_1 Azimuth	Dip	σ_2 Azimuth	Dip	σ_3 Azimuth	Dip	
48	4.5–4.7 Ma[a]	13	34°05′	70°21′	60°	5°	152°	22°	317°	67°	0.96
16	Pliocene	7	33°20.5′	70°17.5′	296°	12°	206°	0°	115°	78°	0.54
17	9.8 Ma[b]	37	32°29′	70°08′	278°	5°	62°	84°	187°	4°	0.62
27	L. Miocene	16	32°47′	70°12.5′	70°	1°	340°	9°	166°	81°	0.88
3	E. Miocene	16	32°45.5′	70°32′	262°	12°	362°	37°	157°	51°	0.98
38	E. Miocene	7	34°07′	70°31′	279°	7°	10°	7°	146°	80°	0.56
39	E. Miocene	8	34°08.5	70°31.5′	227°	22°	322°	12°	78°	65°	0.76
41	E. Miocene	10	34°09′	70°32.5′	218°	9°	328°	66°	125°	22°	0.78
42	E. Miocene	17	34°10′	70°33′	121°	16°	26°	16°	253°	67°	0.80
43	E. Miocene	27	34°12′	70°35′	296°	7°	27°	14°	179°	74°	0.83
49	E. Miocene	18	34°12.5′	70°30.5′	110°	6°	14°	45°	206°	44°	0.72
51	E. Miocene ?	10	34°25′	70°49′	78°	2°	169°	9°	338°	81°	0.62
5	und. Miocene	11	32°48′	70°22.5′	258°	19°	161°	19°	31°	62°	0.59

[a] Ages from Cuadra (1986).
[b] Ages from Cornejo (1991).

Miocene–Pliocene intra-arc zone, which currently is part of the fore arc zone. In the southern area, the measurements of striated fault planes were taken from both the present-day arc and the Miocene–Pliocene arc.

4.1.1. The fore arc zone

4.1.1.1. The northern fore arc zone. In this zone, 197 faults of 13 sites (Table 1) (Fig. 10) were measured in Miocene and Pliocene sediments and intrusive rocks described by Charrier and Munizaga (1979), Thiele (1980), and Charrier et al. (1994). The principal compressional stress direction, σ_1, is close to E–W. The tectonic regime is generally compressional (vertical σ_3) except for two sites where there is a strike-slip regime, with a horizontal σ_3. The R ratio is between 0.59 and 0.98, clearly indicating a Pliocene compressional stress state tending toward a uniaxial stress tensor.

Along the coast, the sediments show little deformation and only a few faults were found. There are measured faults in Miocene marine sediments from the coast, which are compatible with an E–W to NE–SW shortening direction. On the other hand, in one site (Lican site), five faults were measured in Middle Miocene marine sediments (as defined by Valenzuela, 1992). Those present structures are synsedimentary normal faults compatible with a NW–SE extensional direction of deformation. Owing to its synsedimentary character, this deformation is proven to be of the Middle Miocene. Based on its direction and limited development, it is not possible to say if this deformation is due to a regional-scale extensional event. Nevertheless, field work done in other parts of the Chilean Coast, north of this studied area, as in the Caldera Region (Marquardt et al., 1999) show the same E–W synsedimentary extensional deformation during the Miocene, and a superposed E–W Pliocene compressional deformation.

Table 2
Parameters of the deviatoric stress tensors computed from the Pliocene strike-slip faults of the Central Depression and Main Cordillera. Present fore arc zone, central area

Site	Age of unit	ND	Latitude S	Longitude W	Principal stress directions						R
					σ_1 Azimuth	Dip	σ_2 Azimuth	Dip	σ_3 Azimuth	Dip	
TRAHU	Miocene	18	40°18′	72°15′	102°	16°	195°	11°	319°	70°	0.56
MELLI	M. Miocene	13	40°14′	72°13′	87°	11°	332°	64°	181°	23°	0.91
CAUN	295 Ma[a]	14	40°08′	72°15′	95°	24°	286°	65°	187°	4°	0.90

[a] Age from Munizaga et al. (1984).

Table 3
Parameters of the deviatoric stress tensors computed from the Pliocene faults of the Central Depression and Main Cordillera. Present intra-arc zone, central area

Site	Age of unit	ND	Latitude S	Longitude W	Principal stress directions						R
					σ_1 Azimuth	Dip	σ_2 Azimuth	Dip	σ_3 Azimuth	Dip	
X1	8.4 Ma[a]	21	39°35.5′	71°53′	88°	5°	339°	74°	180°	15°	0.33
REL 1	Cr./Mioc. Bath.	38	41°38′	72°19′	263°	5°	173°	7°	30°	82°	0.78
REL 2	Cr./Mioc. Bath.	20	41°30′	72°17′	263°	7°	172°	11°	27°	77°	0.78

[a] Age from Munizaga et al. (1984).

4.1.1.2. The central fore arc zone. In this zone, 45 faults of three sites were measured, 13 faults in Miocene granitic rocks, 18 faults in Miocene turbiditic sediments and 14 faults in Permian intrusive rocks (295 Ma, Munizaga et al., 1984) (Table 2; Fig. 11).

The principal compressional stress direction (σ_1) is E–W. For the CAUN and MELLI sites, the R ratio is close to 1, which corresponds to a compressional strike-slip tectonic regime with a horizontal σ_3 axis. For the third site, TRAHU, the R ratio is 0.56 and corresponds to a compressional regime. The age of this tectonic event is post-Miocene.

4.1.2. The intra-arc zone

4.1.2.1. The central intra-arc zone. In this zone, 79 faults of three sites were measured, 58 faults in Miocene (or Cretaceous to Miocene) batholitic rocks (Munizaga et al., 1988) and 21 faults in Late Miocene intrusive rocks (8.4 Ma, Munizaga et al., 1984) (Table 3; Fig. 11).

In the northern part of this zone, the site X1, with a R ratio 0.33, corresponds to a weak extensional strike-slip regime. The principal compressional stress direction σ_1 is close to E–W (N 088°). In the southern part, both Reloncaví sites, REL1 and REL2 correspond to a uniaxial compressional regime, with an E–W (N 263°) principal compressional stress direction.

4.1.2.2. The southern intra-arc zone. In general, the ages of the rocks are poorly known because these regions are still not well known from a geological point of view (studies and analysis in progress). However, the ages of the studied rocks (Table 4; Fig. 12) are well constrained between Middle Miocene and Early Pliocene, and recently obtained radiometric data allow us to date the deformation (Cembrano, 1998). Cembrano (1998) found that contractional to dextral-oblique ductile deformation zones flanking the Cenozoic magmatic arc were active at around 4.3 Ma. Fault measurements were done in the North Patagonian Batholith (102 faults of six sites). Available Rb–Sr, K–Ar, Ar–Ar dates of intrusive rocks extend from the Cretaceous to the Quaternary (Munizaga et al., 1988; Pankhurst and Hervé, 1994; Cembrano, 1998). In some cases, the ages are unknown (undifferentiated batholith). Four sites were measured in intrusive rocks with Late Miocene to Pliocene Ar–Ar dates (5.5 and 10 Ma, Hervé et al., 1993; and 5.3 and 13.3 Ma, Cembrano, 1998) and two were measured in Patagonian batholitic rocks of uncertain age. The main direction of compression in this case is also close to E–W, the

Table 4
Parameters of the deviatoric stress tensors computed from the Pliocene faults of the Central Depression and Main Cordillera. Present intra-arc zone, southern area

Site	Age of unit	ND	Latitude S	Longitude W	Principal stress directions						R
					σ_1 Azimuth	Dip	σ_2 Azimuth	Dip	σ_3 Azimuth	Dip	
PUYUHUA	5.3 ± 0.3 Ma[a]	21	44°21′	72°34′	268°	2°	359°	13°	168°	77°	0.97
Rio. CISNE	5.5 ± 0.4 Ma[b]	17	44°44′	72°35′	101°	13°	356°	48°	203°	39°	0.95
Pto. CISNE	10 ± 0.3 Ma[b]	20	44°43′	72°34′	237°	17°	90°	70°	331°	10°	0.67
QUEULAT	13.3 ± 0.2 Ma[a]	13	44°29′	72°35′	97°	3°	187°	6°	343°	83°	0.30
Pte FALLA	un. Patag. Bath	16	44°22′	72°35′	268°	19°	65°	70°	175°	7°	0.96
AYSEN	un. Patag. Bath	15	45°19′	72°42′	253°	6°	349°	45°	157°	45°	0.34

[a] Ages from Cembrano (1998).
[b] Ages from Hervé et al. (1993).

Table 5
Parameters of the deviatoric stress tensors computed from the Quaternary and Plio-Quaternary faults of the Central Depression and Main Cordillera. Present fore arc zone, northern area

Site	Age of unit	ND	Latitude S	Longitude W	Principal stress directions						R
					σ_1 Azimuth	Dip	σ_2 Azimuth	Dip	σ_3 Azimuth	Dip	
18	Pleistocene	6	33°36′	70°22.5′	338°	25°	242°	13°	127°	62°	0.76
25	Pleistocene	7	33°33.5′	71°34.5′	5°	2°	275°	4°	120°	85°	0.79
47	2.8–3.9 Ma[a]	21	34°05′	70°21′	23°	0°	114°	86°	293°	4°	0.51
48	4.5–4.7 Ma[a]	13	34°05′	70°21′	180°	10°	276°	33°	75°	56°	0.70
16	Pliocene	8	33°20.5′	70°17.5′	13°	21°	110°	17°	236°	62°	0.67
17	9.8 Ma[b]	7	32°29′	70°08′	37°	4°	307°	11°	148°	79°	0.91
19	M. Miocene	7	33°36′	70°22.5′	359°	18°	99°	28°	239°	56°	0.50
3	E. Miocene	10	32°45.5′	70°32′	161°	4°	315°	85°	71°	2°	0.97
41	E. Miocene	12	34°09′	70°32.5′	27°	5°	291°	48°	122°	42°	0.86
13	Cret./Tertiary	5	33°15′	71°08,5′	203°	18°	306°	33°	89°	51°	0.60

[a] Ages from Cuadra (1986).
[b] Ages from Cornejo (1991).

directions of σ_1 being between ENE–WSW (N 237°) and WNW–ESE (N 101°). In most cases, the tectonic regime is found to be compressional, in some cases, it is a strike-slip compressional regime. The R ratio is between 0.67 and 0.97.

4.2. The Quaternary event

The main results for the Quaternary event are found in Tables 5–9 and Fig. 9.

4.2. The fore arc zone

4.2.1.1. The northern fore arc zone. From the Coastal Range to the Main Cordillera, the ages of sediments and rocks studied (Table 5) were from the limit of the Cretaceous/Tertiary until the Pleistocene but only half of the sites are found in Pliocene–Quaternary rocks. All sites are located in the fore arc zone (96 faults of 10 sites). There have not yet been studies in the magmatic arc zone.

In the majority of sites, stress is compressional with σ_1 horizontal, and σ_3 vertical. R ratio is between 0.5 and 1, the regime therefore experienced uniaxial compression. In only two sites, σ_3 is horizontal and the tectonic regime is strike-slip compressional. The principal direction of stress, σ_1, is N–S to NNE–SSW (N 009°). From the 10 sites studied, the existence of this stress in half of the sites dated from the Pliocene to the Quaternary shows clearly the pre-Quaternary age of the compression (site 47: 2.8–3.9 Ma and site 48: 4.5–4.7 Ma, both by K/Ar dating from Cuadra, 1986). The other sites are in Miocene rocks.

In the Coastal Zone, the few outcrops of

Table 6
Parameters of the deviatoric stress tensors computed from the Quaternary and Plio-Quaternary faults of the Central Depression. Present fore arc zone, central area

Site	Age of unit	ND	Latitude S	Longitude W	Principal stress directions						R
					σ_1 Azimuth	Dip	σ_2 Azimuth	Dip	σ_3 Azimuth	Dip	
ESPERANZA	Pleistocene	6	37°50′	72°23′	359°	4°	90°	12°	250°	77°	0.10
VICTORIA	Pleistocene	3	38°12′	72°20′	40°	–	–	–	–	–	–
FRESIA 1	Pleistocene	37	41°11′	73°22′	209	0°	299°	1°	104°	88°	0.40
FRESIA 2	Pleistocene	13	41°11′	73°22′	26	16°	285°	34°	138°	52°	0.19
BRAUN	Pleistocene	12	41°20′	73°19′	48	11°	313°	23°	160°	64°	0.85
ANCUD 1	Pleistocene	10	41°51′	73°49′	17	30°	172°	57°	280°	11°	0.06
ANCUD 2	Pleistocene	20	41°52′	73°50′	29	2°	120°	29°	296°	61°	0.34
VOLCAN A.	Pleistocene	24	41°51′	72°40′	210	2°	300°	9°	105°	81°	0.40
LAJAS	Pleistocene	12	41°55′	73°52′	341	3°	77°	60°	249°	30°	0.01
ANCUD 3	25.6 ± 0.7 Ma[a]	8	41°51′	73°49′	156	6°	247°	13°	42°	76°	0.16

[a] Age from Stern and Vergara (1992).

Table 7
Parameters of the strain from the Quaternary normal faults of the Coastal Cordillera. Present fore arc zone, central area

Site	Age of unit	ND	Latitude S	Longitude W	Principal stress directions						R
					σ_1 Azimuth	Dip	σ_2 Azimuth	Dip	σ_3 Azimuth	Dip	
ARAUCO Pen.	Pleistocene	6	37°30′	73°19′	–	–	–	–	256°	–	–

Quaternary (and/or Plio-Quaternary) rocks have little deformation and only a few faults are observed. Some 3 km to the east of San Antonio, sandy sediments from the Pleistocene are overthrusted by granite forming the substratum (site 25). Analysis of fault plane measurements allowed for determining a N–S horizontal σ_1 stress tensor (N 005°). The regime is uniaxial compressional.

4.2.1.2. The central fore arc zone. The ages of rocks in which measurements were taken (Table 6) (121 faults of nine sites) range from the Late Oligocene (rhyodacite from Ancud, Chiloé Island, dated in 25.6 ± 0.7 Ma by Stern and Vergara, 1992) to the Pleistocene.

In the majority of sites from the Central Depression (80%), the stress is compressional (σ_1 is horizontal, σ_3 is vertical) with a NNE–SSW direction. In Esperanza (Fig. 9), a Pleistocene site measured in Quaternary terrace sediments (Moreno and Varela, 1985), the R ratio is close to 0, which in this case shows a radial compressional regime (a revolution ellipsoid with $\sigma_1 \cong \sigma_2$). This can be explained by one of the following, the limited cohesion of Quaternary sediments (alluvial terrace), the superficial deformation (without the weight of a column of sediments on top) or the proximity of the valley. In Victoria, the three measured faults do not allow for calculating tensor stress, indicating only the displacement direction along the fault plane.

In Ancud, two sites (Ancud1 and Ancud2) were measured in a Quaternary conglomerate glacial drift (Fuerte San Antonio Drift considered Pleistocene by Heusser and Flint, 1977). In Ancud1, north of Ancud, the regime is strike-slip uniaxial extensional ($R = 0.06$); in Ancud2, south of Ancud, the regime is compressional to radial compressional ($R = 0.34$).

In Fresia and Nueva Braunau, the same Quaternary glacial drift is also affected by a compressional (BRAUN, $R = 0.85$) to radial compressional (FRESIA 1, $R = 0.40$ and FRESIA 2, $R = 0.19$) stress regime.

In the Arauco Peninsula, in the Coastal Zone, a plurikilometric and some decametric N–S to NNE–SSW normal faults cut Pleistocene sediments, compatible with an E–W extension (Table 7) (six faults of one site). This is also found along the coast of Northern Chile, although it is not clear whether the deformation represents a regional-scale extensional event or results from co- or post-seismic deformation (works in progress, Lavenu and Marquardt, 1999; Marquardt et al., 1999; Marquardt and Lavenu, 1999).

4.2.2. The intra-arc zone

4.2.2.1. The central intra-arc zone

Along the LOFZ the measured fault striations (208 faults of six sites) were studied on rocks with Miocene to Pleistocene ages: Miocene K/Ar ages of 8.1 Ma (Añique site) from Munizaga et al. (1984); 8.5–

Table 8
Parameters of the deviatoric stress tensors computed from the Quaternary and Plio-Quaternary strike-slip faults of the Main Cordillera. Present intra-arc zone, central area

Site	Age of unit	ND	Latitude S	Longitude W	Principal stress directions						R
					σ_1 Azimuth	Dip	σ_2 Azimuth	Dip	σ_3 Azimuth	Dip	
HORNOPI	3.59 ± 0.01 Ma[a]	51	42°	72°26′	236°	8°	33°	81°	145°	3°	0.37
AÑIQUE	8.1 ± 0.2 Ma[b]	28	39°37′	71°54.5′	238°	12°	34°	76°	147°	5°	0.60
CABURGU	8.5–11.6 Ma[c]	34	39°08.5′	71°45′	228°	14°	137°	2°	41°	76°	0.90
RELONC1	Cr./Mioc. Bath.	29	41°38′	72°19′	221°	2°	124°	71°	312°	19°	0.61
RELONC2	Cr./Mioc. Bath.	42	41°30′	72°17′	231°	9°	58°	80°	321°	1°	0.63

[a] Ages from Cembrano et al. (1996b).
[b] Ages from Munizaga et al. (1984).
[c] Ages from Munizaga et al. (1988).

Table 9
Parameters of the deviatoric stress tensors computed from the Quaternary and Plio-Quaternary faults of the Main Cordillera. Present intra-arc zone, southern area

Site	Age of unit	ND	Latitude S	Longitude W	Principal stress directions						R
					σ_1 Azimuth	Dip	σ_2 Azimuth	Dip	σ_3 Azimuth	Dip	
PUYUHUAPI	1.6 Ma[a]	16	44°21′	72°34′	52°	6°	202°	83°	321°	3°	0.65
Pto CISNE	10 ± 0.3 Ma[b]	7	44°43′	72°34′	175°	23°	288°	43°	66°	38°	0.63
QUEULAT	13.5 Ma[a]	10	44°29′	72°35′	213°	27°	118°	8°	12°	62°	0.75

[a] Ages from Cembrano (1998).
[b] Ages from Hervé et al. (1993).

11.6 Ma (Caburgua site) from Munizaga et al. (1988); Pliocene rocks of 3.59 Ma (Hornopirén site) from Cembrano et al. (1996b), and Pleistocene outcrops of the Volcán Apagado (Alarcón, 1995) (Table 8).

The most recent stress field obtained from the pyroclastic deposits of the Volcán Apagado is close to a compressional radial regime with an R ratio of 0.40.

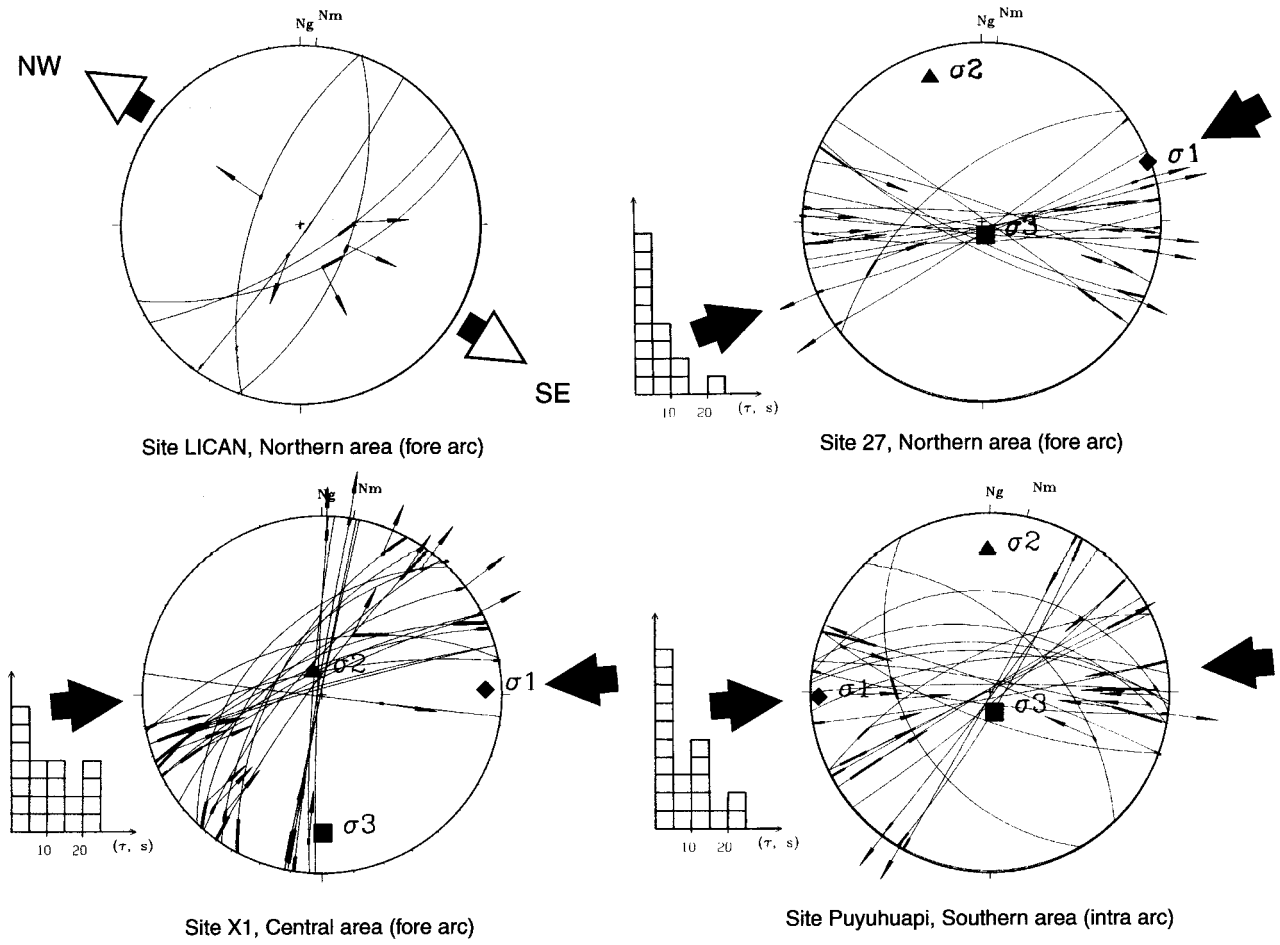

Fig. 8. Main examples of slip vector data from Neogene faults of the Chilean Central Depression and the Main Cordillera. Arrow attached to fault traces corresponds to the measured slip vectors (Wulff stereonet, lower hemisphere). Thick segments on the fault traces and histograms show deviations between measured (s) and predicted (τ) slip vectors on each fault plane. Convergent large arrows give azimuths of the computed maximum principal stress σ_1 direction. Histograms (Nd, τs) represent the distribution of the angular deviation between measured (s) and predicted (τ) slip vectors.

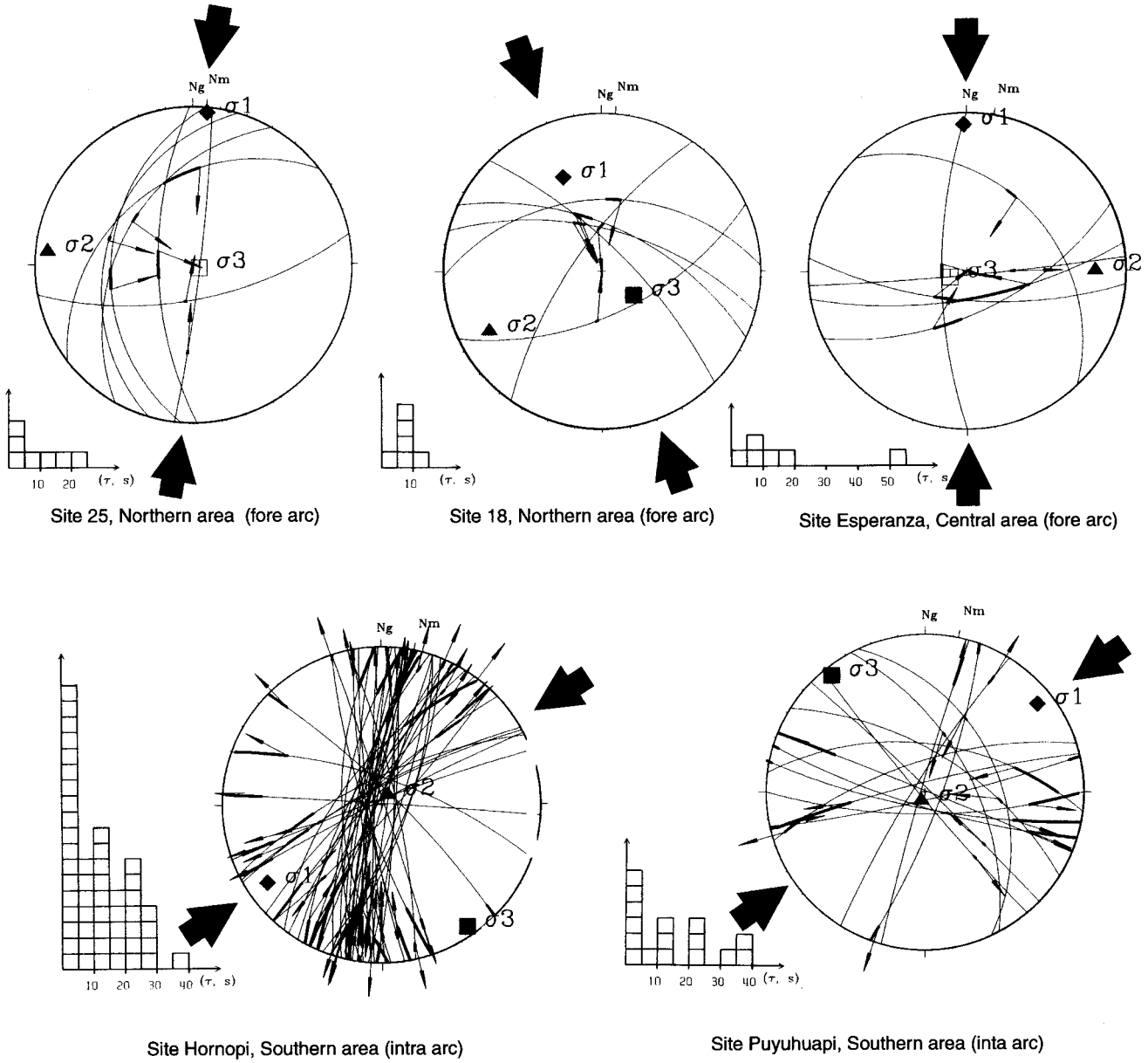

Fig. 9. Main examples of slip vector data from Quaternary faults of the Chilean Central Depression and the Main Cordillera. Symbols as in Fig. 8.

The Late Pliocene Hornopirén site (Hornopi) yields transpressional stress tensors (with σ_1 and σ_3 horizontal) with directions of σ_1 close to NE–SW. This site is close to a pure strike-slip regime where $R = 0.37$.

The sites of Añique and Reloncavi correspond also to a strike-slip regime where R is 0.60–0.63.

4.2.2.2. The southern intra-arc zone

Along the LOFZ, the ages of studied outcrops (Table 9) range from the Middle Miocene (13.5 and 10 Ma, respectively from Cembrano, 1998, and Hervé et al., 1993) to the Quaternary. One $^{40}Ar/^{39}Ar$ age of 1.6 Ma was obtained on weakly deformed biotites (Cembrano, 1998). This age pre-dates the brittle deformation.

In two of the studied sites (Puyuhuapi and Puerto Cisnes, 23 faults), the tectonic regime is tranpressional: σ_1 and σ_3 are horizontal and the R ratio is close to 0.63. In the Queulat site some faults (10 faults) are compatible with a compressional tectonic regime. On average, the direction of σ_1 is N–S to NE–SW.

5. Regional stress pattern

In the Chilean Andes, between 33°S and 46°S, Neogene and Quaternary rocks are affected by a brittle

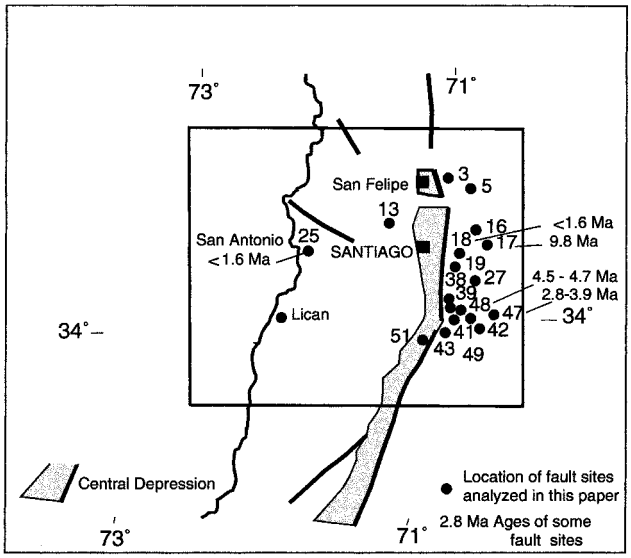

Fig. 10. Location of fault sites analyzed in this paper, Northern Zone. Stippled pattern: Central Depression.

deformation that is weakly developed but widespread. Analysis of the brittle deformation found on the coast, along the Central Depression and the Liquiñe–Ofqui Fault Zone documents the existence of two tectonic events.

The Pliocene event is characterized by a generalized compressional tectonic regime that can be observed in the present fore arc and intra-arc zones (Fig. 13): σ_1 trends E–W, σ_2 trends N–S, and σ_3 is vertical. The state of stress is such that $\sigma_1 > \sigma_2 > \sigma_3$.

During the Quaternary a partition of the deformation can be noted, with the existence of two states of different stress (Fig. 14):

- in the fore arc zone, σ_1 trends N–S to NNE–SSW, σ_2 trends E–W, and σ_3 is vertical.
- in the intra-arc zone, a compressional strike-slip deformation occurs (transpression) and σ_1 trends NE–SW, σ_3 trends NW–SE, and σ_2 becomes vertical.

In the coastal site of the Arauco Peninsula, the Quaternary regime is extensional and of an ~E–W direction. This deformation characterizes the westernmost portion of the continental fore arc, close to the trench axis (~80 km). This deformation does not appear to be directly linked to boundary forces due to the convergence, but could be the consequence of coseismic crustal bending with subduction-related earthquakes. It could be topographic accommodation to the uplift of this part of the coast (body force due to topography): σ_3 becomes E–W-trending, σ_2 trends N–S, and σ_1 is vertical. This phenomenon is also found in other zones of the Chilean coast (La Serena–Coquimbo, Caldera, Mejillones).

The partition of the deformation across the plate

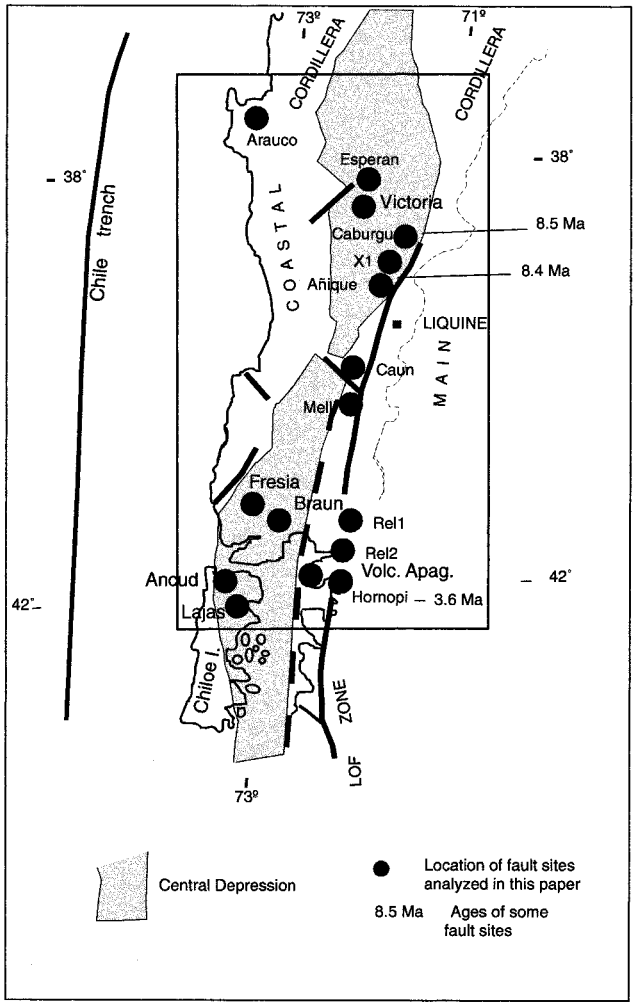

Fig. 11. Location of fault sites analyzed in this paper, Central Zone. Stippled pattern: Central Depression.

boundary zone shows (Fig. 15) that the tectonic regime of the Quaternary is more complex than previously recognized (e.g. Dewey and Lamb, 1992). It does not correspond to the general stress field model predicted numerically by Coblentz and Richardson (1996) in which a nearly uniform E–W orientation of maximum horizontal compressive stress σ_{Hmax} is predicted. Although, these authors estimate the occurrence of possible rotations near the limits of the plates, which could occur in this case.

As to the possibility of block rotations along the LOFZ, previous studies of paleomagnetism were carried out in diverse sites in the south of Chile with rocks from the Paleozoic to Late Tertiary (Beck, 1988; García et al., 1988; Beck et al., 1990; Cembrano et al., 1992; Rojas et al., 1994). Internal consistency of Pliocene stress directions over the large area covered by this study and their random distribution throughout suggests the lack of post-Pliocene significant block rotations along the LOFZ (N $087^\circ \pm 12^\circ$) and in the Main Cordillera east of Santiago (N $086^\circ \pm 27^\circ$). The

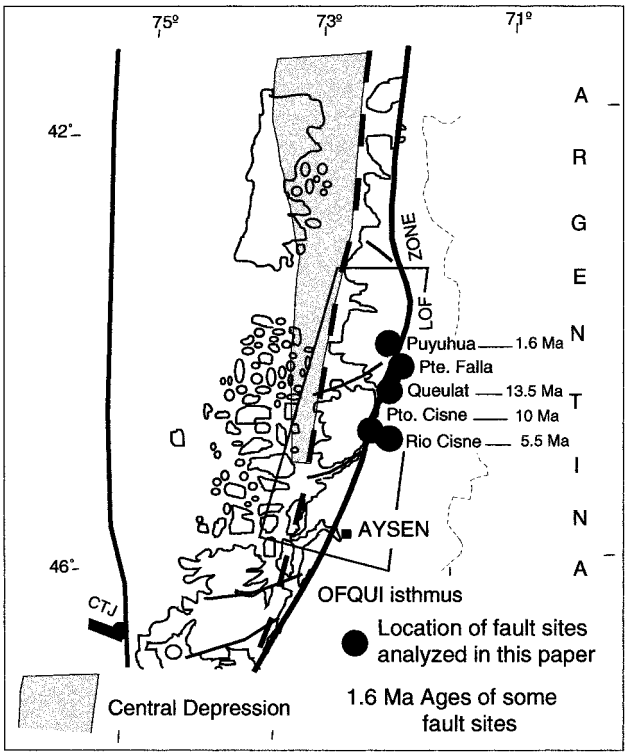

Fig. 12. Location of fault sites analyzed in this paper, Southern Zone. Stippled pattern: Central Depression.

same situation seems to be true for the Quaternary stress directions (N 013° ± 22° in the fore arc, and N 042° ± 20° in the intra-arc). Therefore, the stress directions obtained in this study can be considered as in-situ stress directions within error.

6. Seismicity—neotectonic relationships

Seismological studies have been conducted in the field to the south of 33°S, where the slab changes from a subhorizontal inclination to an inclination of 30° toward the east. Between 28°S and 32°S, the seismic zone is nearly subhorizontal in the flat slab region (Cahill and Isacks, 1985, 1992). This is a zone of strong coupling between the oceanic and continental plates. The surface of the continental plate over this area shows neither active volcanoes nor plateau or Altiplano. The foreland zone is also an area of important surface deformations (e.g. El Tigre fault, Bastias, 1990).

Although between 26°S and 38°S, deep seismicity between the slab and the continental plate has been well studied (Pardo et al., 1996), analysis of shallow crustal seismicity is still scarce (Barrientos and Eisenberg, 1988; Barrientos and Kausel, 1993; Alvarado et al., 1997; Lopez et al., 1997). From a few upper crustal seismic events, the focal mechanism has

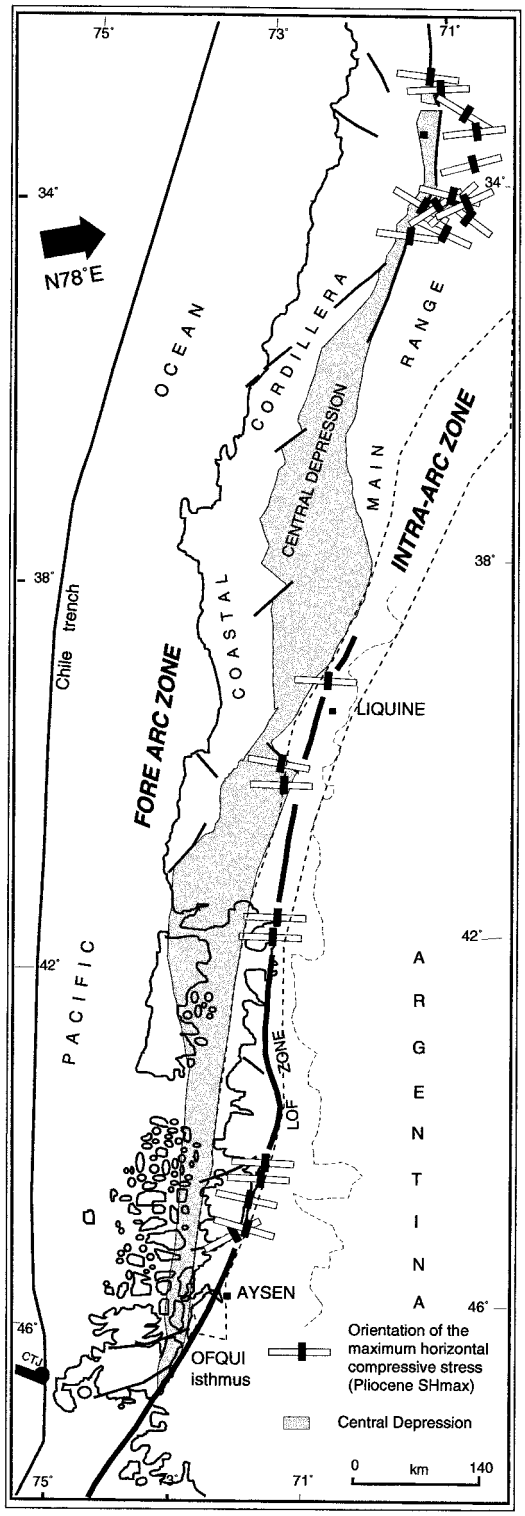

Fig. 13. Principal directions of the maximum horizontal compressional stress σ_{Hmax} deduced from microtectonic analysis of Pliocene faults of the Andes of Central and Southern Chile. In both the fore arc zone (Main Range near Santiago, 34°S, and Central Depression) and intra-arc zone (along the Liquiñe Ofqui Fault Zone), regional compression appears to be E–W, roughly parallel to the direction of convergence (large black arrow) between the two plates.

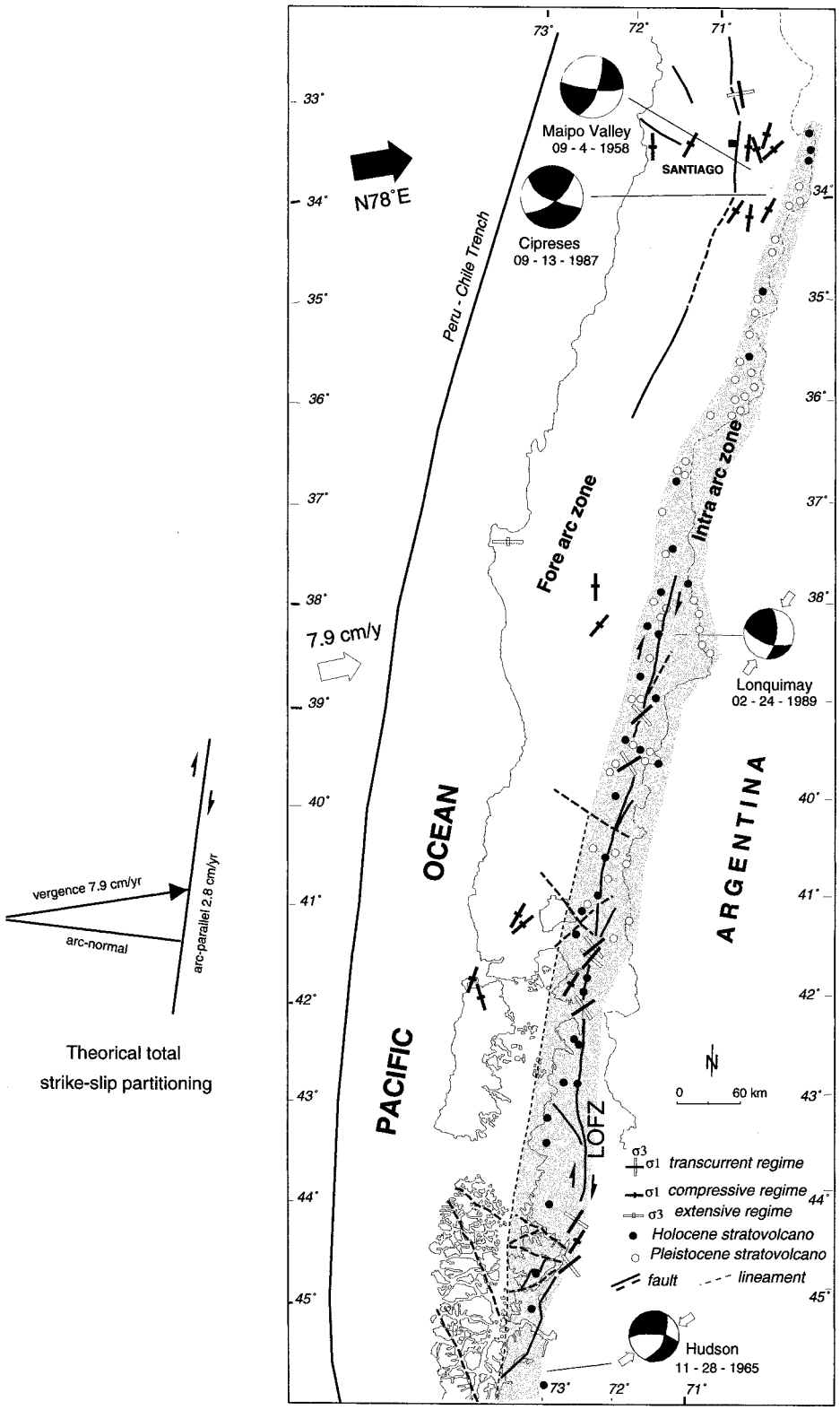

Fig. 14. Principal directions of the maximum horizontal compressional stress σ_{Hmax} deduced from microtectonic analysis of Quaternary faults of the Andes of Central and Southern Chile. During the Quaternary, the deformation was partitioned into two distinctive states of stress. In fore arc zone (Main Range near Santiago, 34°S, and Central Depression) regional compression appears to be N–S. In intra-arc zone (along the Liquiñe Ofqui Fault Zone) the principal transpressional stress direction strikes roughly NE–SW. Left figure shows theoretical total partitioning (convergence rate of 7.9 cm/y) yielding a maximum 2.8 cm/y dextral slip in magmatic arc (cf. McNulty et al., 1998).

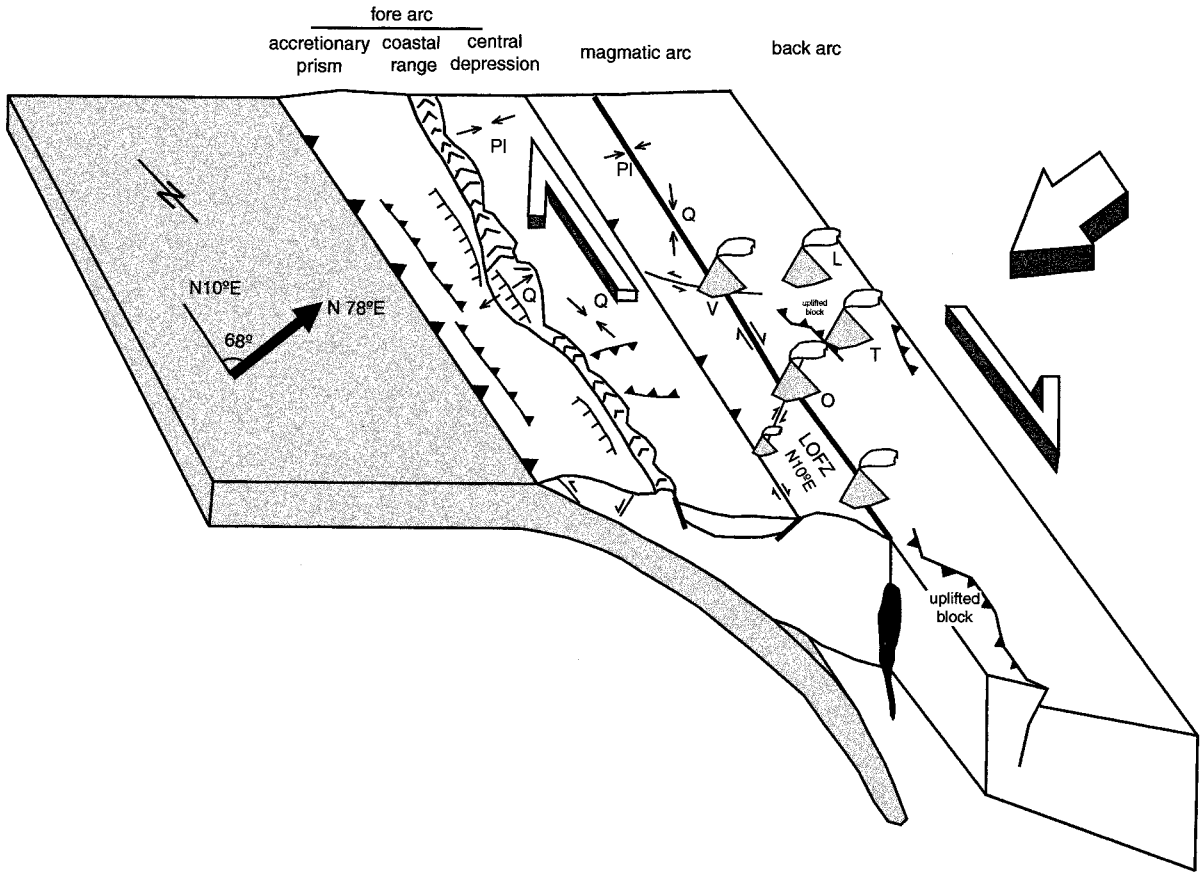

Fig. 15. Kinematic partitioning of overall oblique convergence between Nazca and South American plates, Central and Southern Chile. E–W extension in the western part of the fore arc zone, at the Coast; N–S contraction in the fore arc zone; strike-slip movement concentrated in the magmatic arc Foreland region shows the deformation. Pl: principal Pliocene compressional directions; Q: principal Quaternary compressional and transpressional directions. L: Lanin volcano, V: Villarrica volcano, T: Tronador volcano, O: Osorno volcano.

been calculated (Table 10). Between 33°S and 35°S two focal mechanisms allow correlation of the present deformation with neotectonics (Fig. 14). Despite the limited data, Lomnitz (1961) attempted to calculate a solution for the September 4, 1958 earthquake (Santiago region, 33°50′ Latitude S., 70°10′ Longitude W). The solution corresponds to a N 013 77°W sinistral fault. The slip component could not be calculated, but the fault strike conforms with the most prominent lineaments of the zone. No field evidence of surface rupture was found. In the case of the September 13, 1987 earthquake (100 km SE of Santiago, 34°20′ Latitude S., 70°15′ Longitude W.), Barrientos and Eisenberg (1988) calculated a solution compatible with a dextral fault plane (N 027 58° 176°). Based on this, the slip vector implies that σ_1 is contained in a plane striking ≈N 030°, similar to the calculated paleo-stress direction for this region.

In the central zone, in the extreme north of the LOFZ, near the Lonquimay Volcano (38°22.5′S–71°35.5′W), earthquakes were recorded following the December 25, 1988 eruption. The focal mechanism calculated for the February 24, 1989 earthquake (Dziewonski et al., 1990; Barrientos and Acevedo, 1992) is compatible with a N–S-trending dextral strike-slip fault, with a NNE-trending maximum compressional stress axis. This direction is similar to the calculated Quaternary paleo-stress.

In the southern zone, in the extreme south of the LOFZ, near the Hudson Volcano and 25 km to the east of the principal fault trace, a shallow crustal earthquake was recorded on November 28, 1965. According to Chinn and Isacks (1983) and Nelson et al. (1994) the focal mechanism solution is a dextral reverse slip fault trending NNE–SSW which, as for the other regions, is similar to Quaternary paleo-stress.

In relation to seismicity within the zone of study, the majority of known earthquakes occur at a depth of more than 10 km. The difference in orientation between observed σ_{Hmax} and the direction of deformation obtained by means of focal mechanisms can be explained by local and superficial perturbations of

stress that affect data from superficial levels but not data from deeper levels, such as deep earthquakes (Coblentz and Richardson, 1996). However, it has not been possible to demonstrate a relationship between superficial faults and superficial earthquakes (between 5 and 25 km of depth) when the earthquake does not produce a surface rupture (Pardo and Acevedo, 1984).

7. Strike-slip partitioning

It is commonly recognized that partitioning of deformation occurs in a variety of plate tectonic settings. In many orogenic belts, with oblique convergence, deformation is partitioned into coeval strike-slip and thrust faults. According to some authors, stress is partitioned (e.g. Zoback et al., 1987; Rice, 1992; Zoback and Healy, 1992), while according to other authors, strain is partitioned (e.g. Oldow et al.,1990; Molnar, 1992; cf. Tikoff and Teyssier, 1994 for further explanation). Transpression can be described as a combination of simple shear and pure shear, and it is either wrench dominated or pure-shear dominated, on the basis of the orientation of the instantaneous strain axis (Fossen and Tikoff, 1993; Teyssier et al., 1995; Tikoff and Saint Blanquat, 1997).

In the case of central and southern Chile, the angle between the direction of convergence of the Nazca Plate (~N 79°) and the margin of the South American plate at the level of the Chilean coast and/or the LOFZ (strike ca. N 010° ± 10°) is 69° ± 10° (which is considered to have been constant over the past 5–10 Ma), at a velocity of 7.9 cm/y (DeMets et al., 1994; Tamaki, 1999).

In order to assess deformation partitioning in the context of available models, two stress fields, Pliocene and Quaternary, have to be considered separately. For this analysis we assume that the obtained maximum principal stress direction (σ_1) is approximately parallel to the maximum horizontal axis of the incremental strain ellipsoid. (i) Field analysis of stress for the Pliocene shows that the maximum horizontal compressional stress axis has an average direction of N 086° ± 27° in the fore arc zone and an average direction of N 087° ± 12° in the intra-arc zone. In case of convergence obliquity and partitioning of the deformation as it is demonstrated in Sumatra (Bellier and Sébrier, 1994), and according to Teyssier et al. (1995), the direction of maximum compressional stress bisects the angle between plate motion vector and normal to plate margin, respectively here N 079° and N 100° ± 10°. In the zone of study this direction would then be ∽N 090° ± 10°, very close to the N 086° and N 087° average directions found in the field. (ii) Concerning the Quaternary event, field data and stress field analysis show that the maximum horizontal compressional stress has an average direction of N 013° ±22° in the fore arc zone and N 042° ± 20° in the intra-arc zone (along the LOFZ in particular). Within the fore arc, this somewhat unexpected direction trends roughly parallel to the plate boundary, here N 010° ± 10°. In the intra-arc zone the average direction of the stress axis (N 042° ± 20°) is oblique to both the plate boundary and the LOFZ. It is obvious that neither the direction of σ_1 of the fore arc nor the direction of σ_1 of the arc can be readily explained in terms of Teyssier et al. (1995) analysis of bulk transpressional deformation. In their kinematic model of convergence the direction of σ_1 for homogeneously distributed transpression can lie at most at 45° with respect to the plate boundary zone (for a slip vector parallel to the plate boundary, i.e. strike-slip deformation, which is not the case). Furthermore, in the general case of oblique convergence, even if deformation is fully partitioned (i.e. there is a plate-boundary-parallel discrete zone of simple shear accommodating all the strike-slip components of motion) σ_1 would be orthogonal to the plate margin away from the zone and lying at 45° within the zone of simple shear: this is not the case either. Therefore, there must be other variables that control the geometry of stress across the southern Andes plate boundary zone. We further address this in the discussion.

As the convergence angle did not change much between Miocene and Quaternary, this parameter alone does not explain the change of direction of σ_1 from nearly E–W to almost N–S. However, an important change in velocity is noted from 3 Ma (from 8.4 to 7 mm/y), both perpendicular and tangential to the trench (Engebretson et al., 1986; Engebretson, written communication).

During the Pliocene, the direction of the maximum tectonic compressional stress was E–W, and the degree of plate-slip-vector partitioning was weak. This deformation corresponded in the Central Andes, and in the northwestern Patagonian Andes of Argentina, to the Pliocene tectonic event (posterior to the Quechua period) linked with the increasing of the convergence

Table 10
Earthquake parameters

Date	South lat.	West long.	Prof. km	Mg (mb)	Mg (Ms)	Fault strike	Dip	Slip angle
09-04-58[a]	−33°83.00	−70°16.00	–	–	6.9	193°	77°30′	–
11-28-65[b]	−45°77.00	−72°90.00	33	5.4	6.0	–	–	–
09-13-87[c]	−34°20.31	−70°15.00	6.7	5.6	5.9	27°	58°	176°
02-24-89[d]	−38°38.00	−71°58.00	–	–	5.3	9°	70°	150°

[a] Lomnitz (1961).
[b] Chinn and Isacks (1983).
[c] Barrientos and Eisenberg (1988).
[d] Barrientos and Acevedo (1992).

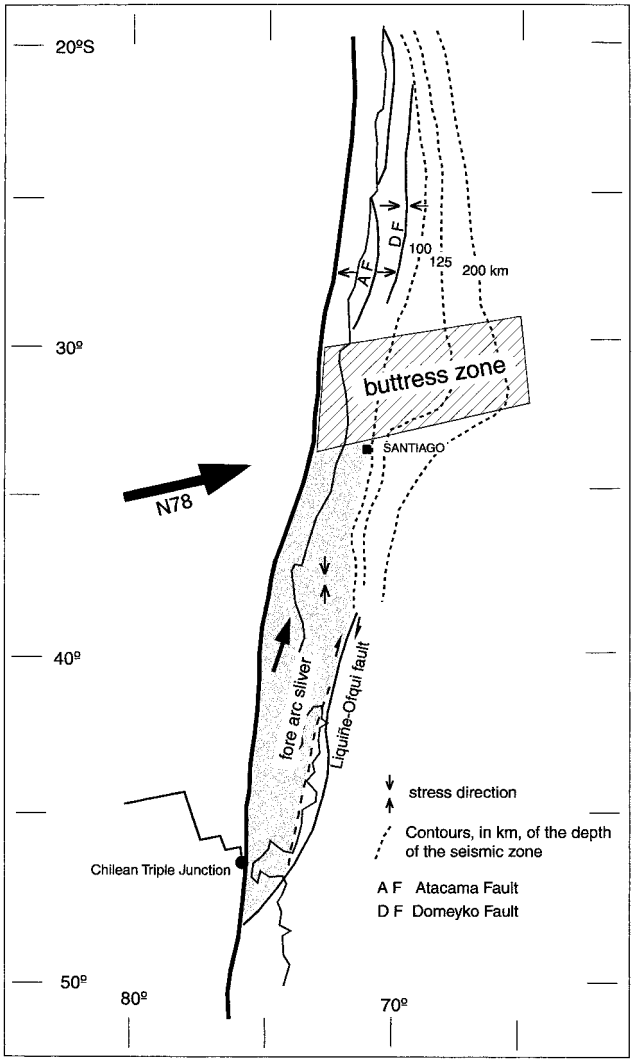

Fig. 16. Potential north-trending motion of the fore arc sliver. Because of the Buttress Zone and the change of the subduction geometry, this part of the fore arc is prevented to freely move northward. North of this buttress zone, N–S compressional deformation is not documented. On the contrary, E–W compressional deformation developed along the Domeyko Fault System (Niemeyer, 1984; Jolley et al., 1990). As in other parts of the Chilean coast, E–W extensional deformation is documented along the Atacama Fault System.

rate between anomalies 5 and 3 (Lavenu et al., 1989; Lavenu and Mercier, 1991; Mercier et al., 1992; Noblet et al., 1996; Diraison et al., 1998). During the Quaternary (post-2 Ma), the tectonic regime has been mainly characterized by N–S compressional tectonics in the Central depression (fore arc) and by strike-slip movements in the intra-arc and along the LOFZ, which implies a remarkable change from the Pliocene stress field. This can be partly explained by a strong and usually ignored effect of the plate-slip-vector partitioning.

In Argentina, to the east of the volcanic arc and the Main Cordillera, a Quaternary deformation is noted, with open folds facing east in the intramontane valley between the Frontal Cordillera and the PreCordillera, and reverse faults facing east with seismic activity in the PreCordillera (Kadinsky-Cade et al., 1985; Costa et al., 1997). In the Sierras Pampeanas there is a thick-skinned crustal shortening facing east along N–S faults (Costa and Vita-Finzi, 1996). Further to the north there is an important deformation of reverse dextral faults with E–W shortening along the active El Tigre fault (Siame et al., 1996). To the south of 35°S no seismicity or active faults have been noted (Chinn and Isacks, 1983; Jordan and Allmendinger, 1986). The Sierras Pampeanas and the Sub-Andean Zone disappear in this region, as well as the flat slab zone. The Main Chilean Cordillera comes in direct contact with the rigid block of the undeformed Argentine basement (Fig. 1). Active deformations seem to be restricted to the fore arc zone and, in particular, the volcanic arc zone. But this deformation is very weak and we have noted only some reverse faults in the Middle Quaternary deposits of the Central Depression and we have nowhere found active faults.

Although the observed directions of shortening are not compatible with those predicted by simple kinematic models (e.g. Teyssier et al., 1995), partitioning of oblique convergence may be responsible for the N–S compression within the fore arc sliver (Fig. 16). In fact, strike-slip partitioning favours a potential northward displacement of the coastal sliver. Northward motion is also enhanced by the collision of successive segments of the Chile Ridge from 14 Ma (e.g. Nelson et al., 1994). According to Beck (1991) and McCaffrey (1992), the kinematics of fore arc deformation not only depends on the angle of relative plate convergence but also on the geometry of the plate boundary, which is assumed to be straight in most kinematic models. Convergent margins that are concave towards the subducting plate should experience margin-parallel shortening because the fore arc zone is prevented from freely moving in the direction of the strike-slip component of overall oblique convergence (Fig. 16). Beck (1991) calls this the 'buttress effect'. In contrast, fore arc regions that are convex towards the subducting plate should experience margin-parallel extension as has been demonstrated for several active subduction zones (e.g. McCaffrey, 1992; Dumont et al., 1997).

The 'buttressed' northward motion due to the geometry of the plate margin of the coastal sliver may not be the only cause of the observed N–S compression. Another source of potential buttressing of northward motion can also be the abrupt change in the slab dip at ~33°S from nearly 30° to subhorizontal. It is noteworthy that the N–S compression has only been found south of 33°S, where the Central Depression starts.

8. Conclusion

The study of recent brittle deformation in the fore arc and intra-arc zones in the Andes of Southern Chile between 33° and 46°S allows us to demonstrate the existence of a partition of maximum horizontal compressive stress (σ_{Hmax}) directions.

Subsequent to the ductile Mio-Pliocene deformation in the LOFZ, two episodes of brittle deformation characterized by faults and/or micro-faults owing to discontinuous shear occurred:

- during the Pliocene, prior to 3.6–2.8 Ma, a compressional tectonic event occurred, characterized by an E–W σ_{Hmax} within the entire zone of study;
- during the Quaternary, after 2.8–1.6 Ma, two different states of stress are evident; one of a N–S to NNE–SSW direction in the fore arc zone, the other of a NE–SW direction, in the volcanic arc zone along the LOFZ.

The E–W Pliocene compression appears directly linked to a rapid convergence regime and an apparently important coupling between both the continental and oceanic plates.

The asperities or irregularities on the descending plate do not seem to affect the Central Depression, the intra-arc zone nor the back arc zone. In addition, it is difficult to relate these morpho-tectonic features to the arrival of ridges (e.g. Juan Fernandez Ridge, von Huene et al., 1997).

The N–S Quaternary compression in the fore arc, linked to a slower convergence regime with a certainly weaker coupling, can be also explained by different factors such as the geometry of the plate margin and/or abrupt changes in subduction geometry.

The fact that Quaternary deformation is weak in both the fore arc and arc regions between 33° and 46°S can be explained by the accommodation of large amounts of plate convergence within the Benioff zone through large-magnitude earthquakes, such as the Valdivia 1960 event. This earthquake accommodated slip equivalent more than 500 years of convergence (e.g. Plafker and Savage, 1970).

Acknowledgements

The present study was part of a current collaboration program between IRD (ex ORSTOM) and the Departamento de Geología, Universidad de Chile. CODELCO Chile, through 'Proyecto Geodinámico El Teniente' funded our field work in Central Chile in 1994. Fondecyt projects 1931096 and 1950497 funded field work in Southern Chile between 1993 and 1998. Students G. Arancibia and G. Vargas are thanked for their help in the field. Professor Sergio Barrientos participated in several discussions in the early stages of this work. Reviewers Richard Allmendinger and Brendan McNulty helped to significantly improve the text. This is UR6 'Resources, environement, dévelopement', IRD contribution.

References

Alarcón, B., 1995. Geología del area comprendida entre los 41°45′–42°05′ latitud sur y 72°25′–72°50′ longitud oeste, Provincias de Llanquihue y Palena, X Región. Thesis, University of Chile.

Alvarado, P., Barrientos, S., Vera, E., 1997. Sismicidad y estructura de la corteza en la región cordillerana de Chile central. VIII° Congreso Geológico Chileno, vol. 1, pp. 615–615.

Anderson, E.M., 1951. The Dynamics of Faulting and Dyke Formation with Applications to Britain. Oliver & Boyd, Edinburgh 206 pp.

Aubouin, J., Audebaud, E., Debelmas, J., Dollfus, O., Dresh, J., Faucher, B., Mattauer, M., Mégord, F., Peredes, J., Savoyat, E., Thiele, R., Vicante, J.C., 1973. De quelques problèmes géologiques et géomorphologiques de la Cordillère des Andes. Revue de Géographie physique et de Géologie dynamique (2)XV, 207–216.

Barazangi, M., Isacks, B.L., 1976. Spatial distribution of earthquakes and subduction of the Nazca plate beneath South America. Geology 4, 686–692.

Barrientos, S., Acevedo, A.P., 1992. Seismological aspects of the 1988–1989 Lonquimay (Chile) volcanic eruption. Journal of Volcanology and Geothermal Research 53, 73–87.

Barrientos, S., Eisenberg, A., 1988. Secuencia sísmica en la zona cordillerana al interior de Rancagua. 5° Congreso Geológico Chileno, Santiago, vol. II, pp. F121–F132.

Barrientos, S., Kausel, E., 1993. Características de la sismicidad andina superficial en la zona central de Chile. VI° Jornada chilena de Sismología e Ingeniería Antisísmica, Santiago.

Bastias, H.E., 1990. Discontinuidades tectónicas a la latitud de 32° sur y su importancia en la hipótesis de evolución de Precordillera. 10° Congreso Geológico Argentino, San Juan, vol. II, pp. 407–411.

Beck, M.E., Burmester, R.F., Garcia, A., Rivano, S., 1990. Paleomagnetic results from Cretaceous rocks in the Llaillay–San Felipe–Puteando region: implications for block rotations in the Andean forearc. Revista Geológica de Chile 17, 115–130.

Beck, M.E., Rojas, C., Cembrano, J., 1993. On the nature of buttressing in margin-parallel strike-fault systems. Geology 21, 755–758.

Beck, M.E., 1983. On the mechanism of tectonic transport in zones of oblique subduction. Tectonophysics 93, 1–11.

Beck, M.E., 1988. Analysis of Late Jurassic–Recent paleomagnetic data from active plate margins of South America. Journal of South American Earth Sciences 1, 39–52.

Beck, M.E., 1991. Coastwise transport reconsidered: lateral displacements in oblique subduction zones, and tectonic consequences. Physics of the Earth and Planetary Interiors 68, 1–8.

Bellier, O., Sébrier, M., 1994. Relationship between tectonism and volcanism along the Great Sumatran Fault Zone deduced by Spot image analyses. Tectonophysics 233, 215–231.

Bevis, M., Isacks, B., 1984. Hypocentral trend surface analysis: Proving the geometry of Benioff zones. Journal of Geophysical Research 89, 6153–6170.

Bott, M.H.P., 1959. The mechanics of oblique slip faulting. Geological Magazine 97, 109–117.

Cahill, T., Isacks, B., 1985. Shape of the subducted Nazca plate. EOS, Transactions of the American Geophysical Union 66, 299.

Cahill, T., Isacks, B., 1992. Seismicity and shape of the subducted Nazca plate. Journal of Geophysical Research 97, 17503–17529.

Carey, E., Brunier, B., 1974. Analyse théorique et numérique d'un modèle élémentaire appliqué à l'étude d'une population de failles.

Comptes Rendus de l'Académie des Sciences, Paris, D 269, 891–894.

Carey, E., 1979. Recherche des directions principales de contraintes associées au jeu d'une population de failles. Revue de Géographie physique et Géologie dynamique 21, 57–66.

Cembrano, J., Hervé, F., 1993. The Liquiñe–Ofqui fault zone: a major Cenozoic strike slip duplex in the Southern Andes. Second International Symposium of Andean Geodynamics, Oxford, extended abstracts, pp. 175–178.

Cembrano, J., Beck, M.E., Burmester, R.F., Rojas, C., Garcia, A., Hervé, F., 1992. Paleomagnetism of Lower Cretaceous rocks from east of the Liquiñe–Ofqui fault zone, southern Chile: evidence of small in-situ clockwise rotations. Earth and Planetary Science Letters 113, 539–551.

Cembrano, J., Hervé, F., Lavenu, A., 1996a. The Liquiñe–Ofqui fault zone: a long-lived intra-arc fault system in southern Chile. Tectonophysics 259, 55–66.

Cembrano, J., Schermer, E., Lavenu, A., Hervé, F., Barrientos, S., McClelland, B., Arancibia, G., 1996b. Nature and timing of Cenozoic intra-arc deformation, southern Chile. 3° International Symposium of Andean Geodynamics, St Malo, France, extended abstracts, pp. 311–314.

Cembrano, J., Lavenu, A., Arancibia, G., Sanhueza, A., Reynolds, P., 1997. Coeval transpressional and transtensional magmatic arc tectonics in the southern Andes. VIII° Congreso Geológico Chileno, vol. III, pp. 1613–1616.

Cembrano, J., 1992. The Liquiñe–Ofqui fault zone (LOFZ) in the Province of Palena: field and microstructural evidence of a ductile–brittle dextral shear zone. Comunicaciones 43, 3–27.

Cembrano, J., 1998. Kinematics and timing of intra-arc deformation at the Southern Andes plate boundary zone. PhD thesis, University of Dalhousie.

Charrier, R., Munizaga, F., 1979. Edades K–Ar de vulcanitas cenozoicas del sector cordillerano del rio Cachapoal (34°15′ de latitud sur). Revista Geológica de Chile 7, 41–51.

Charrier, R., Wyss, A.R., Flynn, J.J., Swisher, C.C., III, Spichiger, S., Zapatta, F., 1994. Nuevos antecedentes estratigráficos y estructurales para las formaciones Coya–Machali y Abanico, entre 33°50′ y 35° Cordillera Principal chilena. 7° Congreso Geológico Chileno, Concepción, vol. II, pp. 1316–1319.

Chinn, D.S., Isacks, B.L., 1983. Accurate source depths and focal mechanisms of shallow earthquakes in western south America and in the New Hebrides island arc. Tectonics 2, 529–563.

Cisternas, M.E., Frutos, J., 1994. Evolución tectónico-paleogeográfica de la cuenca terciaria de los Andes del sur de Chile (34°30′–40°30′ lat. S). VII° Congreso Geológico Chileno, vol. 1, pp. 6–12.

Coblentz, D.D., Richardson, R.M., 1996. Analysis of the South American intraplate stress field. Journal of Geophysical Research 101, 8643–8657.

Cornejo, P., 1991. Geology, mineral compositions and magmatic gradients of a zoned pluton: La Gloria pluton, Central Chilean Andes. MSc thesis, Stanford University.

Costa, C., Vita-Finzi, C., 1996. Late Holocene faulting in the southeast Sierras Pampeanas of Argentina. Geology 24, 1127–1130.

Costa, C., Lavenu, A., Diederix, H., Cortes, J., Gardini, C., Ramos, V., 1997. Quaternary deformations in Chile and Argentina along 32–33° south latitude (abs). Geological Society of America Annual Meeting, Abstracts with Programme, A442.

Cuadra, P., 1986. Geocronología K–Ar del yacimiento El Teniente y áreas adyacentes. Revista Geológica de Chile 27, 3–26.

DeMets, C., Gordon, R., Argus, D., Stein, S., 1994. Effect of recent revisions to the geomagnetic reversal time scale on estimates of current plate motions. Geophysical Research Letters 21, 2191–2194.

Dewey, J.F., Lamb, S.H., 1992. Active tectonics of the Andes. Tectonophysics 205, 79–95.

Diraison, M., Cobbold, P., Rossello, E., Amos, A., 1998. Neogene dextral transpression due to oblique convergence across the Andes of northwestern Patagonia, Argentina. Journal of South American Earth Sciences 11, 519–532.

Dumont, J.F., Alvarado, A., Guillier, B., Lavenu, A., Martinez, C., Ortlieb, L., Poli, J.T., Labrousse, B., 1997. Coastal morphology as related to geodynamics in Western Ecuador: preliminary results. In: Late Quaternary Coastal Tectonics, London, O-07. INQUA Commission on Neotectonics and Geological Society, London.

Dziewonski, A.M., Ekstrom, G., Woodhouse, J.H., Zwart, G., 1990. Centroid-moment tensor solutions for January–March 1989. Physics of the Earth and Planetary Interiors 59, 233–242.

Engebretson, D.C., Cox, A., Gordon, R.G., 1986. Relative motions between oceanic and continental plates in the Pacific basin. Geological Society of America, Special Paper, 206, 59 pp.

Fitch, T.J., 1972. Plate convergence, transcurrent faults, and internal deformation adjacent to southeast Asia and the western Pacific. Journal of Geophysical Research 77, 4432–4460.

Forsythe, R.D., Nelson, E.P., 1985. Geological manifestations of ridge collision: Evidence from the Golfo de Penas–Taitao basin, southern Chile. Tectonics 4, 477–495.

Fossen, H., Tikoff, B., 1993. The deformation matrix for simultaneous simple shearing, pure shearing and volume change, and its application to transpression–transtension tectonics. Journal of Structural Geology 15, 413–422.

Garcia, A., Beck, M.E., Burmester, R.F., Hervé, F., Munizaga, F., 1988. Paleomagnetic reconnaissance of the Región de Los Lagos, Southern Chile, and its tectonic implications. Revista Geológica de Chile 15, 13–30.

Hauser, A., 1991. Hans Steffen, precursor del concepto Falla Liquiñe–Ofqui. Revista Geológica de Chile 18, 177–179.

Hervé, F., Thiele, R., 1987. Estado de conocimiento de las megafallas en Chile y su significado tectónico. Comunicaciones 38, 67–91.

Hervé, F., Fuenzalida, I., Araya, E., Solano, A., 1979. Edades radiometricas y tectónicas neógenas en el sector costero de Chiloé, X Región. Actas Cong. Geol. Chileno 2, F1–F18.

Hervé, F., Pankhurst, R., Drake, R., Beck, M., Mpodozis, C., 1993. Granite generation and rapid unroofing related to strike-slip faulting, Aysen, Chile. Earth and Planetary Science Letters 120, 375–386.

Hervé, M., 1976. Estudio geológico de la falla Liquiñe–Reloncaví en el area de Liquiñe; antecedentes de un movimiento transcurrente (Provincia de Valdivia). I° Congreso Geológico Chileno, vol. I, B, pp. 39–56.

Hervé, M., 1977. Geología del área al este de Liquiñe, Provincia de Valdivia, Xa Región. Thesis, University of Chile, Santiago.

Heusser, C., Flint, R., 1977. Quaternary glaciations and environments of northern Isla Chiloé, Chile. Geology 5, 305–308.

Jarrard, R.D., 1986. Relations among subduction parameters. Reviews of Geophysics 24, 217–284.

Jolley, E.J., Turner, P., Williams, G.D., Hartley, A.J., Flint, S., 1990. Sedimentological response of an alluvial system to Neogene thrust tectonics, Atacama Desert, northern Chile. Journal of the Geological Society 147, 769–784.

Jordan, T.E., Allmendinger, R.W., 1986. The Sierras Pampeanas of Argentinas: a modern analogue of Rocky Mountain foreland deformation. American Journal of Science 286, 737–764.

Jordan, T.E., Isacks, B.L., Allmendinger, R.W., Brewer, J.A., Ramos, V.A., Ando, C.J., 1983. Andean tectonics related to geometry of subducted Nazca plate. Geological Society of America Bulletin 94, 341–361.

Kadinsky-Cade, K., Reilinger, R., Isacks, B., 1985. Surface deformation associated with the November 23, 1977, Caucete, Argentina, earthquake sequence. Journal of Geophysical Research 90 (B14), 12691–12700.

Klohn, C., 1955. Informe geológico sobre el volcán Pillanilahue. Corporación de Fomento de la Producción. Unpublished Report.

Klohn, C., 1960. Una zona de inestabilidad estructural con fracturas profundas en los Andes del sur de Chile reactivada en el terremoto del 22 de mayo de 1960. Institute of Investigative Geology. Unpublished Report, 14 pp.

Laugenie, C., 1982. La région des Lacs, Chili méridional. Recherche sur l'évolution géomorphologique d'un piémont glaciaire quaternaire andin. Thèse de Doctorat, University of Bordeaux III.

Lavenu, A., Cembrano, J., 1994. Neotectónica de rumbo dextral en la zona de falla de Liquine–Ofqui: geometría, cinemática y tensor de esfuerzo. 7° Congreso Geológico Chileno, vol. I, pp. 81–85.

Lavenu, A., Mercier, J.L., 1991. Evolution du régime tectonique de l'Altiplano et de la Cordillère Orientale des Andes de Bolivie du Miocène supérieur à l'Actuel. Géodynamique 6, 21–55.

Lavenu, A., Bonhomme, M.G., Vatin-Pérignon, N., DePachtère, P., 1989. Neogene magmatism in the Bolivian Andes between 16°S and 18°S: stratigraphy, and K/Ar geochronology. Journal of South American Earth Sciences 2, 35–47.

Lavenu, A., Noblet, C., Winter, T., 1995. Neogene ongoing tectonics in the Southern Ecuadorian Andes: analysis of the evolution of the stress field. Journal of Structural Geology 17, 47–58.

Lavenu, A., Cembrano, J., Arancibia, G., Déruelle, B., Lopez-Escobar, L., Moreno, H., 1997. Neotectónica transpresiva dextral y volcanismo, Falla Liquiñe–Ofqui, sur de Chile. VIII° Congreso Geológico Chileno, vol. I, pp. 129–133.

Lavenu, A., Marquardt, C., Comte, D., Pardo, M., Ortlieb, L., Monfret, T., 1999. Quaternary extensional deformation and recent vertical motion along the Chilean coast (between 23°S and 47°S). Fourth International Symposium of Andean Geodynamics, extended abstracts, Göttingen (in press).

Lomnitz, G., 1961. A study of the Maipo Valley earthquakes of September 4, 1958. Instituto de Geofísica y Sismología, Santiago, pub. 10, pp. 501–520.

Lopez, G., Hatzfeld, D., Madariaga, R., Barrientos, S., Campos, J., Lyon-Caen, H., Zollo, A., Giannacone, G., Kausel, E., 1997. Microsismicidad en la zona centro-sur de Chile. VIII° Congreso Geológico Chileno, vol. III, pp. 1771–1774.

Marquardt, C., Lavenu, A., 1999. Quaternary brittle deformation in the Caldera area, northern Chile (27°S). Fourth International Symposium of Andean Geodynamics, extended abstracts, Göttingen (in press).

Marquardt, C., Ortlieb, L., Lavenu, A., Guzman, N., 1999. Recent vertical motion and Quaternary marine terraces in the Caldera area, northern Chile (27°S). Fourth International Symposium of Andean Geodynamics, extended abstracts, Göttingen (in press).

McCaffrey, R., 1992. Oblique plate convergence, slip vectors, and forearc deformation. Journal of Geophysical Research 97, 8905–8915.

McNulty, B., Farber, D., Wallace, G., Lopez, R., Palacios, O., 1998. Role of plate kinematics and plate-slip-vector partitioning in continental magmatic arcs: Evidence from the Cordillera Blanca, Peru. Geology 26, 827–830.

Mercier, J.L., Sébrier, M., Lavenu, A., Cabrera, J., Bellier, O., Dumont, J.F., Macharé, J., 1992. Changes in the tectonic regime above a subduction zone of andean type: the Andes of Peru and Bolivia during the Pliocene–Pleistocene. Journal of Geophysical Research 97, 11945–11982.

Molnar, P., 1992. Brace–Goetze strength-profiles, the partitioning of strike-slip and thrust faulting at zones of oblique convergence, and the stress-heat flow paradox of the San Andreas fault. In: Evans, B., Wong, T.F. (Eds.), Fault Mechanics and Transport Properties of Rocks. Academic Press, New York, pp. 435–459.

Moreno, H., Varela, J., 1985. Geología, volcanismo y sedimentos piroclasticos cuaternarios de la región central y sur de Chile. In: Tosso, J. (Ed.), Suelos volcánicos de Chile. Instituto de Investigaciones Agropecuarias, Santiago, pp. 491–526.

Moreno, H., Parada, M.A., 1974. Geología del área de Liquiñe–Neltume y Lago Pirihueico. Unp. Rep., Instituto de Investigación Geológica, Santiago, Chile.

Munizaga, F., Hervé, F., Drake, R., 1984. Geocronología K–Ar del extremo septentrional del Batólito Patagónico en la región de Los Lagos, Chile. 9° Congreso Geológico Argentino, Actas III, pp. 133–145.

Munizaga, F., Hervé, F., Drake, R., Pankhurst, R.J., Brook, M., Snelling, N., 1988. Geochronology of the Lake Region of south-central Chile (39°–42°S). Preliminary results. Journal of South American Earth Sciences 1, 309–316.

Nelson, M.R., Jones, C.H., 1987. Paleomagnetism and crustal rotations along a shear zone, Las Vegas Range, southern Nevada. Tectonics 6, 13–33.

Nelson, E., Forsythe, R., Arit, I., 1994. Ridge collision tectonics in terrane development. Journal of South American Earth Sciences 7, 271–278.

Niemeyer, H., 1984. La megafalla Tucúcaro en el extremo sur del Salar de Atacama: una antigua zona de cizalle reactivada en el Cenozoico. Comunicaciones 34, 37–45.

Noblet, C., Lavenu, A., Marocco, R., 1996. Concept of continuum as opposed to periodic tectonism in the Andes. Tectonophysics 255, 65–78.

Oldow, J.S., Bally, A.W., Avé Lallemant, H.G., 1990. Transpression, orogenic float, and lithospheric balance. Geology 18, 991–994.

Pankhurst, R.J., Hervé, F., 1994. Granitoid age distribution and emplacement control in the North Patagonian Batholith in Aysen (44°–47°S). 7° Congreso Geológico Chileno, vol. II, pp. 1409–1413.

Pardo, M., Acevedo, P., 1984. Mecanismo de foco en la zona de Chile central. Tralka 2, 279–294.

Pardo, M., Comte, D., Monfret, T., Vera, E., Gonzalez, N., 1996. Central Chile seismotectonics and stress distribution along the subducted Nazca plate. III International Symposium on Andean Geodynamics (St Malo, 1996), extended abstracts, pp. 215–218.

Plafker, G., Savage, J.C., 1970. Mechanism of the Chilean earthquakes of May 21 and 22, 1960. Geological Society of America Bulletin 81, 1001–1030.

Rice, J.R., 1992. Fault stress states, pore pressure distributions, and the weakness of the San Andreas fault. In: Evans, B., Wong, T.F. (Eds.), Fault Mechanics and Transport Properties of Rocks. Academic Press, New York, pp. 435–459.

Ritz, J.F., Taboada, A., 1993. Revolution stress ellipsoids in brittle tectonics resulting from an uncritical use of inverse methods. Bulletin de la Société Géologique de France 164, 519–531.

Rojas, C., Beck, M.E., Burmester, R.F., Cembrano, J., Hervé, F., 1994. Paleomagnetism of the Mid-Tertiary Ayacara Formation, southern Chile: counterclockwise rotation in a dextral shear zone. Journal of South American Earth Sciences 7, 45–56.

Sébrier, M., Mercier, J.L., Mégard, F., Laubacher, G., Carey-Gailhardis, E., 1985. Quaternary normal and reverse faulting and the state of stress in the central Andes of southern Peru. Tectonics 4, 739–780.

Siame, L., Sébrier, M., Bellier, O., Bourles, D., Castaño, J.C., Aurojo, M., Yiouf, F., Raisbeck, G.M., 1996. Segmentation and horizontal slip-rate estimation of the El Tigre Fault zone, San Juan Province (Argentina) from Spot image analysis. 3° International Symposium of Andean Geodynamics, St Malo, France, extended abstracts, pp. 239–242.

Solano, A., 1978. Geología del sector costero de Chiloé continental entre los 41°50′ y 42°10′ de latitud sur. Thesis, University of Chile.

Steffen, H., 1944. Patagonia occidental. Las cordilleras patagónicas y sus regiones circundantes. Ed. de la Universidad de Chile, Santiago, vol. 1, 333 pp.

Stern, C., Vergara, M., 1992. New age for the vitrophyric rhyolite–dacite from Ancud (42°S), Chiloé, Chile. Revista Geologica de Chile 19, 249–251.

Sylvester, A.G., 1988. Strike-slip faults. Geological Society of America Bulletin 100, 1666–1703.

Tamaki, K., 1999. Nuvel-1A calculation results. Ocean Research Institute, University of Tokyo. http://manbow.ori.u-tokyo.ac.jp/tamaki-bin/post-nuvella.

Teyssier, C., Tikoff, B., Markley, M., 1995. Oblique plate motion and continental tectonics. Geology 23, 447–450.

Thiele, R., 1980. Hoja Santiago. Carta Geológica de Chile, Escala 1:250 000. Instituto de Investigaciones Geológicas, Santiago, vol. 39, 21 pp.

Tikoff, B., Teyssier, C., 1994. Strain modeling of displacement-field partitioning in transpressional orogens. Journal of Structural Geology 16, 1575–1588.

Tikoff, B., Saint Blanquat, de M., 1997. Transpressional shearing and strike-slip partitioning in the late Cretaceous Sierra Nevada magmatic arc, California. Tectonics 16, 442–459.

Valenzuela, E., 1992. Desplazamientos tectónicos y eustáticos de la Costa central de Chile durante el Neogeno. Comunicaciones 43, 77–88.

von Huene, R., Corvalan, J., Flueh, E.R., Hinz, K., Korstgard, J., Ranero, C.R., Weinrebe, W., CONDOR Scientists, 1997. Tectonic control of the subducting Juan Fernández Ridge on the Andean margin near Valparaiso, Chile. Tectonics 16, 474–488.

Wallace, R.E., 1951. Geometry of shearing stress and relation to faulting. Journal of Geology 59, 118–130.

Zoback, M.D., Healy, J.H., 1992. In situ stress measurements to 3.5 km depth in the Cajon Pass scientific research borehole: implications for the mechanics of crustal faulting. Journal of Geophysical Research 97, 5039–5057.

Zoback, M.D., Zoback, M.L., Mount, V.S., Suppe, J.P., Healy, J.H., Oppenheimer, D.H., Reasenberg, P.A., Jones, L.M., Raleigh, C.B., Wong, I.G., Scott, Oona, Wentworth, C.M., 1987. New evidence on the state of stress of San Andreas fault system. Science 238, 1105–1111.